Polyelectrolyte Brushes with Protein-Like Nanocolloids

Tatiana Popova, Oleg Borisov, Ekaterina Zhulina

Polyelectrolyte brushes with protein-like nanocolloids.

Tatiana O.Popova[1,2], Oleg V.Borisov [3,2,1,*], Ekaterina B.Zhulina [2,*],
[1]St.Petersburg National Research University of Information Technologies, Mechanics and Optics, 197101 St.Petersburg, Russia
[2]Institute of Macromolecular Compounds of the Russian Academy of Sciences, 199004 St.Petersburg, Russia
[3] CNRS, Université de Pau et des Pays de l'Adour UMR 5254, Institut des Sciences Analytiques et de Physico-Chimie pour l'Environnement et les Matériaux, Pau, France

December 8, 2023

Abstract

Electrostatic interaction of ampholytic nanocolloidal particles (NP), which mimic globular proteins, with polyelectrolyte brush is analyzed within mean-field Poisson-Boltzmann approximation. In accordance with experimental findings, the theory predicts that an electrostatic driving force for the particle uptake by the brush may emerge when the net charge of the particle in the buffer and the charge of the brush are of the same sign. The origin of this driving force is change in the ionization state of weak cationic and anionic groups on the NP surface provoked by interaction with the brush. In experimental systems the ionic interactions are complemented by excluded volume, hydrophobic, and other types of interactions that all together control NP uptake by or expulsion from the brush. Here we focus on the NP-brush ionic interactions. It is demonstrated, that deviation between the buffer pH and the NP isoelectric point, considered usually as the key control parameter, does not uniquely determine the insertion free energy patterns. The latter depends also on proportion of cationic and anionic groups in the NP and their specific ionization constants as well as on salt concentration in the buffer. The analysis of the free energy

landscape proves that a local minimum in the free energy inside the brush appears provided the NP charge reversal occurs upon insertion into the brush. This minimum corresponds either to a thermodynamically stable or to a metastable state, depending on the pH offset from the IEP and salt concentration, and is separated from the bulk of the solution by a free energy barrier. The latter, being fairly independent of salt concentration in height, may strongly impede the NP absorption kinetically even when it is thermodynamically favorable. Hence, change reversal is a necessary, but insufficient condition for the uptake of the NPs by similarly charged polyelectrolyte brush.

Keywords: polyelectrolyte brushes, globular proteins, ampholytic nanocolloids, absorption, Poisson-Boltzmann theory, charge reversal.

email: oleg.borisov@uiv-pau.fr

Introduction

Polyelectrolyte (PE) brushes, i.e., arrays of ionically charged macromolecules tethered by one of the terminals to a planar substrate or to the surface of a colloidal particle and immersed in a solvent, remain in the focus of experimental and theoretical research for at least three decades.

Anchoring of ultrathin layers of charged macromolecules at solid-liquid interface is a promising approach for efficient control of adhesive and tribological surface properties,[1–5] as well as aggregative stability of colloidal dispersions.[6–8] The responsiveness of polymer layers to external stimuli, e.g. ionic strength and pH of the solution or applied electrical voltage,[9–12] defines PE brushes as "smart" substrates in tissue engineering. Colloidal PE brushes and self-assembled nanoscale micelles of block-polyelectrolytes are most actively explored for drug and gene delivery, antiviral therapeutics, etc.[13–20]

Furthermore, synthetic PE brushes mimic in many aspects pericellular layers of charged biopolyelectrolytes (glycosaminoglycans).[21–26] Comprehensive study of the well-defined model systems could provide important insights in biolubrication, cell recognition and adhesion, selective molecular transport through biological membranes, etc., occurring in living nature. Ultimately, this understanding may be essential for applying principles of biomimetism in design of novel functional polymer materials with outstanding properties.

Basic theoretical understanding of the fundamental properties of PE brushes, including counterion condensation and coupling between conformation and ionization in pH-sensitive polyelectrolytes, was achieved on the basis of simplified mean-field approach.[8,27–30] These theoretical works essentially motivated pioneering experimental research in this domain.[31–36] After that, a number of experimental works devoted to synthesis and experimental studies of properties of PE brushes grew tremendously (see, e.g. comprehensive reviews[37–39]). More advanced theories based on Poisson-Boltzmann approach enabled deeper insight in structural and nanomechanical properties of PE brushes,[40–44] including those formed by branched PEs.[45] Consistent scaling approach enabled distinguishing between intra- and intermolecular Coulomb repulsions in the brush-forming PE chains and thus to go beyond the mean-field schemes in describing effects of screening of electrostatic interactions in PE brushes.[46] In the past years interaction of PE brushes with globular proteins and their ability to uptake or repel proteins from the solution were actively studied.[23,47–51,53,55,66] Unravelling of mechanisms of the PE brush interactions with (bio)nanocolloids, e.g., globular proteins, is highly important for such applications as protein separation and purification, design of bionanocolloidal reactors, etc., but also for understanding of biological phenomena involving interactions of proteins and viruses with biomacromolecu-

lar brushes decorating cell surfaces.

Electrostatic forces control to a great extent the interactions between charged biomacromolecules, e.g. DNA or glycosaminoglycans and globular proteins in living nature.[22–26] While most of biomacromolecules are negatively charged, proteins are weak polyampholytes, that is, comprise in variable proportion pH-sensitive cationic and anionic groups (amino acid residues) capable of acquiring positive or negative charge over (de)protonation. Under physiological conditions most of proteins are negatively charged, that is, are found above their isoelectric points (IEP). However, as it was evidenced from many experiments,[52–54] electrostatic forces govern binding and complex formation between proteins and charged macromolecules even with a similar (e.g., negative) net charge.

Recent experimental studies[50,51,55–62] were performed on well-defined model systems comprising globular proteins and negatively or positively charged colloidal PE brushes. The presence of electrostatic driving force for the protein uptake by the polyanionic brush not only below, but also above the IEP was confirmed. Similar effects were observed for polycationic brushes and positively charged (below the IEP) proteins.[47] Upon an increase in the ionic strength of the solution the protein absorption in the similarly charged PE brush was suppressed that confirms the electrostatic nature of the driving force for the protein absorption.

Two theoretical models were proposed to explain protein absorption by the similarly charged brush: The first model suggests that the protein negatively charged in the buffer, acquires positive charge inside the negatively charged brush due promoted ionization of the cationic and suppressed ionization of the anionic groups and, therefore, is attracted into the brush by the Coulomb force.[63,64] The second model assumes strong charge-charge correlations and applies to proteins with essentially inhomogeneous distribution of cationic and anionic amino acid residues on the globule surface. In this case oppositely charged "patches" on the globular surface survey as adsorption sites for oppositely charged PE chains,[65–67] that can be also envisioned as formation of a local IPEC.[13] It is anticipated that in general case, both mechanisms driving spontaneous protein absorption by the PE brush both below and above the IEP may be involved.[64]

In our previous studies[68,69] we have systematically studied the effects of the buffer pH_b and salt concentration on the uptake of nanoparticles (NPs) by negatively charged PE brush using a simplified model of NP comprising equal numbers of ionizable cationic and anionic groups on its surface with equal acidic ionization constants, $K_+ = K_-$. The position-dependent differential free energy of the NP insertion into the brush and net particle charge were calculated within the non-linear Poisson-Boltzmann approximation. It was

demonstrated that the shape of the free energy profiles and thus partition of the NPs between the buffer solution and the brush can be efficiently tuned by varying the difference, $\delta pH_b = pH_b - pH_{IEP}$, and changing ionic strength in the solution.

When the pH_b is significantly higher than the pH_{IEP}, the NP is negatively charged in the buffer and retains negative charge inside the brush, thus being expelled from the brush by Coulomb forces. On the contrary, when the pH_b is lower than the pH_{IEP}, the NP in the solution outside the brush has a net positive charge. The magnitude of this positive charge increases as it approaches and enters the brush, since the fraction of positively charged ionized groups on the surface of the NP increases while the fraction of negatively charged ones decreases. The most interesting is the case when the pH_b slightly above pH_{IEP} and the particle in the buffer is negatively charged, but as it enters the brush and approaches the grafting surface, an enhanced ionization of cationic and suppressed ionization of anionic groups leads to the NP charge reversal. This phenomenon is most attractive from the experimental point of view since colloidal PE brushes could retain aggregative stability upon uptake of similarly charged NPs, e.g., globular proteins, and could be exploited for enzymatic colloidal nanoreactors, protein separation and purification, therapeutic proteins delivery, etc.

Hence, the shape of the NP free energy landscape can be most efficiently tuned by variation in environmental conditions, i.e., pH_b deviation from the IEP and salt concentration. However, NPs with different combinations of cationic and anionic groups with their specific ionization constants may exhibit the same IEP. Therefore, as demonstrated in this study, the buffer pH_b deviation from the IEP (at given salt concentration) is not a universal control parameter for the shape of the insertion free energy profiles and thus for the particle uptake/exclusion scenario: The latter may differ for the NPs that have the same IEP, but different combination of cationic and anionic groups with their ionization constants on the particle surface.

An additional contribution to the insertion free energy arises due to the excess osmotic pressure inside the brush. This excess osmotic pressure gives rise to the force repealing NP from the brush. For a given set of the brush parameters (polymerization degree and degree of ionization of the brush forming chains and grafting density) this contribution depends only on salt concentration and particle volume, but not on the electrochemical properties of the NPs.

In ref[70] we have analyzed the full insertion free energy profiles for the BSA with explicit account of the set of all amino acid residues present on the BSA globule surface and contributions of osmotic repulsive and hydrophobic attractive forces. It was demonstrated, that, at equal pH_b deviation above

or below the IEP, the polyanionic brush stronger absorbs BSA than the polycationic brush. In the present publication we consider a model of the NP with variable proportion of cationic and anionic groups on its surface. We examine specifically how this proportion and the values of the ionization constants affect the profiles of the insertion free energy and thus control the NP uptake by or exclusion from the PE brush.

Results and Discussion

Poisson-Boltzmann theory of a PE brush.[40,41]

In this section we summarize results of the theory of strong (not pH-sensitive) PE brush developed in refs,[40,41] in the framework of the non-linear Poisson-Boltzmann approximation which allows unified analytical description of structural and electrical properties of the PE brush at arbitrary salt concentration (including salt-free regime). The brush is formed by strong polyelectrolyte (polyacid) chains with degree of polymerization $\mathcal{N}$ end-tethered to the planar surface. The grafting area per chain (inverse grafting density) is s. The polyelectrolyte chains are assumed to be intrinsically flexible (the monomer unit length is on the order of Kuhn segment, a), with a fraction β of permanently negatively charged monomer units. The brush is immersed into an aqueous solution which contains positively and negatively charged monovalent ions of salt with concentrations (number densities) $c_{b+} = c_{b-} = c_s$ which specify the Debye screening length $\kappa^{-1} = (8\pi l_B c_s)^{-1/2}$. Here $l_B = \frac{e^2}{\epsilon k_B T}$ is the Bjerrum length (e is the elementary charge, ϵ is the dielectric permittivity of the solvent, k_B is the Boltzmann constant, and T is the temperature).

The polyelectrolyte brush gives rise to electrostatic field with the position-dependent Coulomb potential $\Psi(z) \leq 0$, where $z \geq 0$ is distance from the grafting surface and the reference potential value is chosen as $\Psi(z = \infty) = 0$. As demonstrated in refs,[40,41] as long as the polyelectrolytes exhibit linear (Gaussian) entropic elasticity, the reduced electrostatic potential, $\psi(x) \equiv e\Psi(x)/k_B T$, of negatively charged (polyanionic) brush, can be presented as

$$\psi_{in}(z) = \frac{z^2 - H^2}{H_0^2} + \psi_{in}(H), \qquad 0 \leq z \leq H \tag{1}$$

where H is the total thickness of the brush (cut-off of the polymer density profile), and H_0 is the characteristic length

$$H_0/a = \sqrt{\frac{8}{3\pi^2}} \mathcal{N} \beta^{1/2} \tag{2}$$

The potential value $\psi_{in}(H)$ in eq 1 depends on the calibration and is chosen to ensure continuity of the potential at the edge of the brush, $\psi_{in}(H) = \psi_{out}(H)$.

In the solution outside of the brush, at $z \geq H$, the electrostatic potential $\psi_{out}(z)$ coincides with the potential created by a uniformly negatively charged planar surface with charge number density $\tilde{Q}$ that can be presented as[41]

$$\psi_{out}(z) =$$

$$-2\ln\left[\frac{(\kappa\tilde{\Lambda}+\sqrt{(\kappa\tilde{\Lambda})^2+1}-1)+(\kappa\tilde{\Lambda}-\sqrt{(\kappa\tilde{\Lambda})^2+1}+1)e^{-\kappa(z-H)}}{(\kappa\tilde{\Lambda}+\sqrt{(\kappa\tilde{\Lambda})^2+1}-1)-(\kappa\tilde{\Lambda}-\sqrt{(\kappa\tilde{\Lambda})^2+1}+1)e^{-\kappa(z-H)}}\right] \quad (3)$$

Here

$$\tilde{\Lambda} = \frac{1}{2\pi l_B|\tilde{Q}|} \quad (4)$$

and $\tilde{Q}$ is the residual charge per unit area of the brush found from the condition

$$\tilde{Q} = \int_0^H \rho(z)dz$$

with the brush net charge density $\rho(z)$ obtained by combining eq 1 with the Poisson equation

$$\frac{d^2\psi_{in}(z)}{dz^2} = -4\pi l_B\rho(z) \quad (5)$$

The latter specifies the number density of monomer units in the brush, $c_p(z)$, as

$$\beta c_p(z) = -\rho(z) + c_s\exp(-\psi_{in}(z)) - c_s\exp(\psi_{in}(z)) \quad (6)$$

Here, the second and the third terms on the r.h.s. in eq 6 define the local concentrations of mobile cations and anions of added salt inside the brush, respectively. Normalization, $\int_0^H c_p(z)dz = \mathcal{N}/s$, of the monomer density profile $c_p(z)$ specified by eqs 5,6 enables finding the brush thickness H.

In **Figure 1**, the reduced potential profiles $\psi(z)$ are plotted for varied $\mathcal{N}$ (at constant dimensionless salt concentration $C_s = c_s a^3$ and grafting area $S = s/a^2$ per polyion), varied $S = s/a^2$ (at constant $\mathcal{N}$ and C_s), and varied C_s (at constant $\mathcal{N}$ and $S = s/a^2$) in panels a, b, and c, respectively. As one can see from **Figure 1a**, the brush thickness H scales proportionally to $\mathcal{N}$, but the magnitude of the potential change across the brush $\psi(z = \infty) - \psi_{in}(z = 0)$ is fairly independent of $\mathcal{N}$. The zoomed profiles of the electrostatic potential in the vicinity of the grafting surface for varied the degree of polymerization $\mathcal{N}$ are shown in the **Figure S1**. An increase in grafting density, a^2/s, leads to additional stretching of the brush-forming

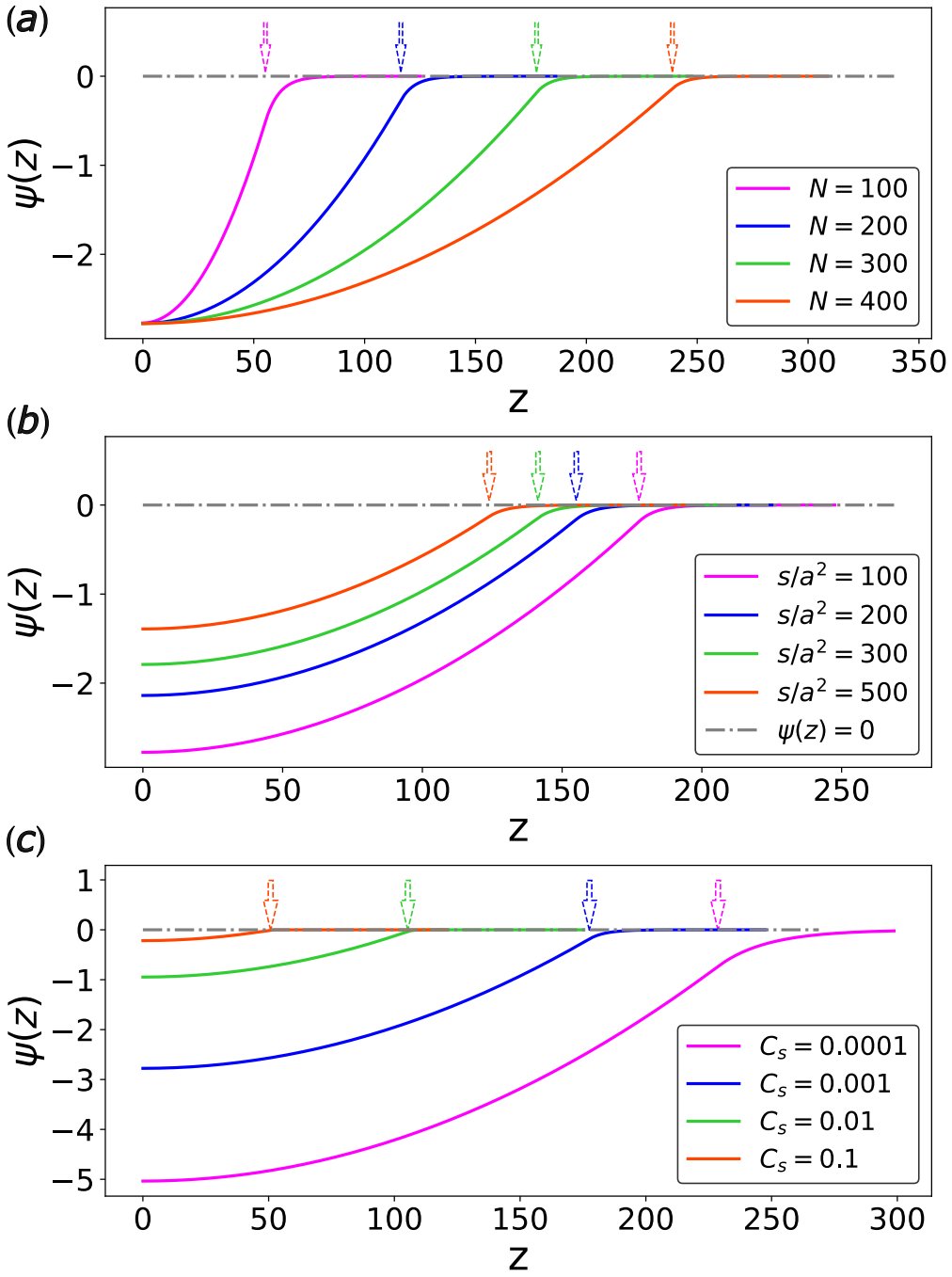

Figure 1: Electrostatic potential of the anionic polyelectrolyte brush as a function of the distance from the grafting surface z and varied degree of polymerization (varied $\mathcal{N}$), $l_B = a$ for $C_s = c_s a^3 = 0.001$, $S = s/a^2 = 100$, $\beta = 0.5$ (a), varied grafting density (varied surface area per chain $S = s/a^2$), $l_B = a$ for $C_s = c_s a^3 = 0.001$, $\mathcal{N} = 300$, $\beta = 0.5$ (b) and varied salt concentration $C_s \equiv c_s a^3$, $l_B = a$ for $\mathcal{N} = 300$, $S = s/a^2 = 100$, $\beta = 0.5$ (c). The brush boundary, $z = H$, is indicated by the arrows.

chains (at increase in H) with concomitant increase in the magnitude of the negative potential $\psi_{in}(z)$ inside the brush (**Figure 1b**). Finally, an increase in salt concentration leads to the brush contraction (the decrease in H) with concomitant decrease in the magnitude of the (negative) potential $\psi(z)$ both inside and outside the brush. This is caused by partial screening of Coulomb interactions between charged monomer units in the PE brush, since the concentration of counterions inside the brush increases. Hence, the brush electrostatic potential $\psi(z)$ is controlled by $\{\mathcal{N}, \beta, S = s/a^2\}$ and C_s, and variations in any of these parameters affect the NP - PE brush interaction (**Figure 1c)**. In the considered here case of strong ('quenched') PE brush the potential $\psi(z)$ is not affected by the buffer pH_b. We remark, that positive electrostatic potential profiles in the brush formed by cationic polyelectrolyte chains with fraction β of positively charged monomer units can be obtained from those presented in **Figure 1** for the polyanionic brush by mirror reflection with respect to the z-axis.

Hence, the spatial distribution of the electrostatic potential $\psi(z)$ created by the brush is controlled by the polymerization degree N and the fraction β of charged monomer units in the brush-forming chains, surface area S per chain and salt concentration C_s in the buffer. In the following we consider the NP interacting with a polyanionic brush with the following representative parameters: $\mathcal{N} = 300$, $\beta = 0.5$, $S = s/a^2 = 100$. We assume that $l_B = a$, which leads to the proportionality factor ≈ 5 between molar concentration and volume fraction $C_s = c_s a^3$ of the salt ions.

Model of the protein-like NP.

To model a protein molecule in its compact globular conformation, we consider an ampholytic NP that comprises N_+ ionogenic groups (sites) capable of acquiring positive (elementary) charge upon protonation, and N_- monomer units capable of acquiring negative (elementary) charge upon dissociation of a hydrogen ion. The total number of ionizable groups on the NP surface is

$$N_\Sigma = N_+ + N_- \tag{7}$$

The fraction of cationic ionizable groups on the NP surface is defined as

$$f_+ = \frac{N_+}{N_+ + N_-} = \frac{N_+}{N_\Sigma} \tag{8}$$

and $f_- = 1 - f_+$ is the fraction of negatively charged groups on the surface of NP.

The charge of the NP (measured in the elementary charge units) in the buffer with given pH_b can be expressed as

$$\frac{Q_b}{N_\Sigma} = \frac{Q(z=\infty)}{N_\Sigma} = f_+\alpha_{b+} - (1-f_+)\alpha_{b-} \tag{9}$$

with the respective ionization degrees of cationic and anionic residues in the bulk of the solution given by

$$\alpha_{b+} = (1 + K_+/[H^+]_b)^{-1} \equiv (1 + 10^{pH_b - pK_+})^{-1} \tag{10}$$

and

$$\alpha_{b-} = (1 + [H^+]_b/K_-)^{-1} \equiv (1 + 10^{pK_- - pH_b})^{-1} \tag{11}$$

Here, $pH_b \equiv -\log[H^+]_b$ with $[H^+]_b$ being molar concentration of H^+ ions in the buffer solution, and we ascribe the acidic ionization constant K_- to anionic groups and the ionization constant K_+ to cationic groups, and use standard notations $pK_+ \equiv -\log K_+$, $pK_- \equiv -\log K_-$.

The isoelectric point, pH_{IEP}, corresponds to pH_b at which the NP charge in the buffer vanishes, $Q_b = 0$. Equations 9, 10, 11, and the condition $Q_b = 0$ define the relationship between the isoelectric point (pH_{IEP}), the ionization constants and the fraction of cationic groups on the NP surface as

$$\frac{1 + 10^{pK_- - pH_{IEP}}}{1 + 10^{pH_{IEP} - pK_+}} = \frac{1 - f_+}{f_+} \tag{12}$$

By solving eq 12 with respect to pH_{IEP}, one obtains the expression for pH_{IEP} in explicit form,

$$pH_{IEP} = pK_- + \log\left[\frac{2f_+ - 1}{2(1-f_+)}\frac{K_-}{K_+} + \sqrt{\left(\frac{K_-}{2K_+}\right)^2 \cdot \left(\frac{2f_+ - 1}{1 - f_+}\right)^2 + \frac{f_+}{(1-f_+)} \cdot \frac{K_-}{K_+}}\right] \tag{13}$$

Importantly, different combinations of $\{f_+, pK_+, pK_-\}$ may correspond to the same isoelectric point pH_{IEP}. It is convenient to introduce new variables as

$$pK^{(m)} = \frac{pK_+ + pK_-}{2}$$

and

$$\Delta = \frac{pK_+ - pK_-}{2}$$

so that

$$pK_+ = pK^{(m)} + \Delta$$

and

$$pK_- = pK^{(m)} - \Delta$$

.

Obviously, pH_{IEP} is an increasing function of f_+ and, in the particular case of $pK_+ = pK_- = pK^{(m)}$, one finds

$$pH_{IEP}|_{pK_+=pK_-=pK^{(m)}} = pK^{(m)} + \log\frac{f_+}{1-f_+} \tag{14}$$

As follows from the equation 12, in the case of equal numbers of cationic and anionic groups, $f_+ = 0.5$, the equation for the pH_{IEP} takes the simple form:

$$pH_{IEP}|_{f_+=0.5} = \frac{pK_+ + pK_-}{2} \equiv pK^{(m)} \tag{15}$$

to provide pH_{IEP} independent of Δ.

For NP with approximately equal numbers of anionic and cationic groups, expansion of eq 13 with respect to small parameter $|f_+ - 0.5| \ll 1$ gives

$$pH_{IEP} \approx pK^{(m)} + (10^{\Delta}+1)(2f_+ - 1)/\ln 10 \approx$$

$$\begin{cases} pK^{(m)} + (2f_+ - 1)/\ln 10, & pK_- > pK_+ \\ pK^{(m)} + 2(2f_+ - 1)/\ln 10, & pK_- = pK_+ \\ pK^{(m)} + 10^{\Delta}(2f_+ - 1)/\ln 10, & pK_+ > pK_- \end{cases} \tag{16}$$

As one can see from **Figure S2**, and in accordance with eq 16, all the $pH_{IEP}(f_+)$ curves for $pK_- > pK_+$ have small slopes at $f_+ = 0.5$ which are virtually independent of $\{pK_+, pK_-\}$. This follows from the fact that in this case both cationic and anionic groups are uncharged around pH_{IEP}. Consequently, the charge of the particle is weakly affected by changes in the fraction of positively charged groups on the surface or the difference between the ionization constants. The larger pK_- is compared to pK_+, the larger the pH_b range where the protein-like particle has virtually no charge.

On the contrary, the slope of the $pH_{IEP}(f_+)$ curves at $f_+ = 0.5$ in the case of $pK_+ > pK_-$ sharply increases as the difference $2\Delta = (pK_+ - pK_-)$ grows. At $f_+ \to 1$ the $pH_{IEP}(f_+, pK_+, pK_-)$ curve approach that for $\{pK'_+, pK'_-\} = \{pK_+, pK_+\}$, i.e. for the case $pK_+ = pK_- = pK'_+$, whereas at $f_+ \to 0$ the $pH_{IEP}(f_+, pK_+, pK_-)$ curve approaches that plotted for $\{pK'_+, pK'_-\} = \{pK_-, pK_-\}$, i.e. for the case $pK_+ = pK_- = pK'_-$. Note that this is true for all cases $pK_+ > pK_-$. The same trends are demonstrated in **Figure S3** in which we present 3D - plots of pH_{IEP} as function of the ionization constants $\{pK_+, pK_-\}$ for selected values of f_+.

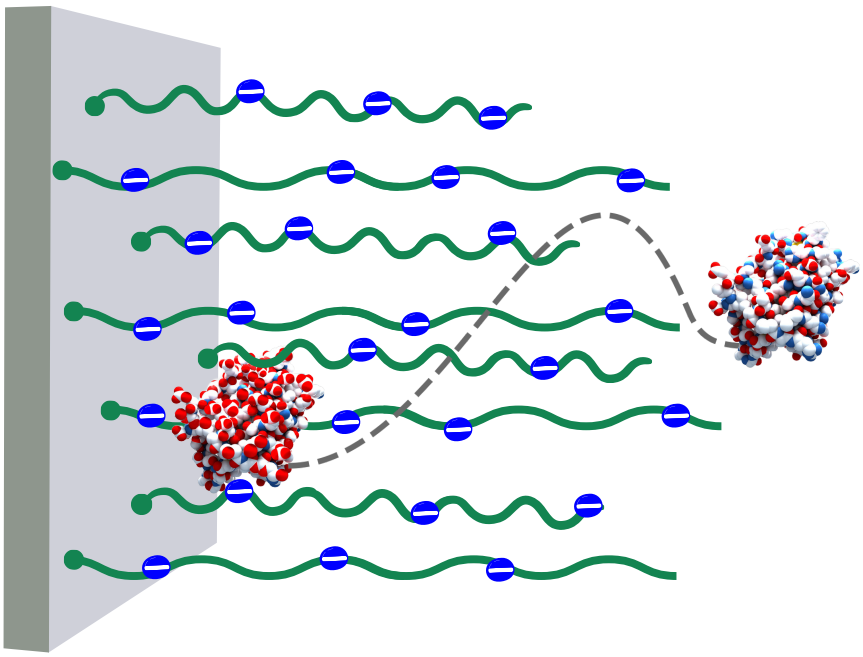

Figure 2: Scheme of the process of interaction of NP with planar polyanionic brush at $pH > pH_{IEP}$. The ionization free energy profile is represented by a gray dashed line. The nanoparticle has positive, negative and uncharged areas on its surface, marked in red, blue and white, respectively.

As follows from eqs 9, 10 and 11, the NP charge Q_b in the buffer depends on the deviation of the buffer pH_b from the IEP. Below we use the parameter

$$\delta pH_b \equiv pH_b - pH_{IEP}$$

to quantify this deviation. The NP charge in the buffer is $Q_b \leq 0$ at $\delta pH_b \geq 0$ and $Q_b \geq 0$ at $\delta pH_b \leq 0$, respectively.

NP interacting with the PE brush.

Insertion free energy and the NP charge

The system under study is schematically depicted in the **Figure 2**. Insertion of the ampholytic nanocolloidal particle from the bulk of the solution into PE brush leads to the change in ionization degree of both basic and acidic monomer groups. The respective free energy change can be presented[68,69] as

$$\Delta F_{ion}(z)/N_\Sigma k_B T = f_+ \ln\left(\frac{1-\alpha_+(z)}{1-\alpha_{b+}}\right) + (1-f_+)\ln\left(\frac{1-\alpha_-(z)}{1-\alpha_{b-}}\right) \quad (17)$$

where $\alpha_+(z)$, α_{b+}, $\alpha_-(z)$, α_{b-} are the respective degrees of ionization of basic and acidic groups on the surface of NP placed at distance z from the grafting surface and in the bulk of the solution (at $z = \infty$), respectively. We remark that eq 17 is a particular case of more general equation derived in ref[69] for the case when the particle surface is decorated by multiple types of cationic and anionic groups.

The corresponding ionization degrees of cationic and anionic groups depend on the local pH as

$$\alpha_+(z) = (1+K_+/[H^+(z)])^{-1} \equiv (1+10^{pH(z)-pK_+})^{-1} = (1+\frac{1-\alpha_{b+}}{\alpha_{b+}}\exp(\psi(z)))^{-1} \tag{18}$$

and

$$\alpha_-(z) = (1+[H^+(z)]/K_-)^{-1} \equiv (1+10^{pK_- - pH(z)})^{-1} = (1+\frac{1-\alpha_{b-}}{\alpha_{b-}}\exp(-\psi(z)))^{-1} \tag{19}$$

Here $[H^+(z)]$ is the local concentration of hydrogen ions at distance z from the grafting surface,

$$[H^+(z)] = [H^+]_b \exp(-\psi(z)) \tag{20}$$

that specifies local $pH(z) = -\log[H^+(z)])$, $pH_b \equiv pH(z = \infty) = -\log[H^+(z = \infty)]$.

The net charge of the NP depends on its position z with respect to the grafting surface and can be expressed as

$$\frac{Q(z)}{N_\Sigma} = f_+\alpha_+(z) - (1-f_+)\alpha_-(z) \tag{21}$$

Hence, as follows from eqs 17, 18, 19, 20 and 21, the position-dependent insertion free energy and net charge of the particle are controlled by the electrostatic potential $\psi(z)$ created by the brush.

Below we use

$$\lambda(z) = \exp(\psi(z)) \tag{22}$$

to describe spatial distribution of electrostatic potential inside, $\psi_{in}(z), z \in [0, H)$, and outside, $\psi_{out}(z), z \in [H, \infty)$, the brush. According to our calibration of the potential, $\lambda(z = \infty) = 1$ and $\lambda(z) \leq 1, z \in [0, \infty)$.

Depending on the sign of $\Delta F_{ion}(z \leq H)$, the NPs are either absorbed by the PE brush (if $\Delta F_{ion} < 0$), or expelled from the brush (if $\Delta F_{ion} > 0$). Obviously, at $pH_b < pH_{IEP}$, when the NP is charged positively (oppositely to the brush), uptake of the NPs by the brush is thermodynamically favorable and driven by Coulomb attraction of opposite charges. The situation is

more delicate at $pH_b > pH_{IEP}$, when the particle in the buffer is negatively charged. As long as hydrogen ions are distributed between PE brush and solution unevenly according to eq 20, lower electrostatic potential inside the brush, $\psi(z) \leq 0$, indicates that local concentration of H^+ ions inside the brush is larger than in the bulk of the solution. As a result, the degree of ionization of basic residues inside polyanionic brush is higher, while the degree of ionization of acidic residues is lower than in the bulk of the solution (eqs 18 and 19). Then the sign of $\Delta F_{ion}(z)$ is determined by the balance between re-ionization free energies of basic and acidic monomer units (the first and the second terms in eq 17, respectively).

Below we focus primarily on the case of $pH_b \geq pH_{IEP}$, that is, $\delta pH_b \geq 0$, when the NP in the bulk of the solution is charged negatively, $Q_b \leq 0$, i.e., similarly to the brush. Because the electrostatic potential $\psi(z)$ created by the brush is a negative monotonically increasing function of z vanishing at $z \to \infty$ (i.e., monotonically increasing in absolute value upon approaching the grafting surface), the net charge $Q(z)$ of the NP monotonically increases upon approaching the grafting surface and, depending on the sets of parameters $\{N_\pm, K_\pm\}$, $\{C_s, \delta pH_b\}$ may either remain negative or invert its sign to positive at some distance z^* from the grafting surface, so that

$$Q(z = z^*) = 0 \tag{23}$$

The position z^* can be found from the equation:

$$\psi(z^*) = -\frac{\delta pH_b}{\log(e)} \tag{24}$$

which implies that $pH(z^*) = pH_{IEP}$. By taking the derivative of the free energy $\Delta F_{ion}(z)$, eq 17, with respect to z it is straightforward to demonstrate that $\Delta F_{ion}(z)$ exhibits a maximum in the point of the charge inversion, $z = z^*$,

$$\left(\frac{\partial \Delta F_{ion}(z)}{\partial z}\right)_{z=z^*} = 0; \left(\frac{\partial^2 \Delta F_{ion}(z)}{\partial z^2}\right)_{z=z^*} < 0; \Delta F_{ion}(z^*) > 0$$

(see ref.[69] for detailed discussion).

Particle with equal numbers of cationic and anionic sites

Consider first interaction of the brush with the NP comprising equal numbers of cationic and anionic groups, $f_+ = f_- = 0.5$. We remind, that, according to eq 15, in this case $pH_{IEP} = (pK_+ + pK_-)/2$ irrespectively of $\Delta = (pK_+ - pK_-)/2$. Below we examine the effects of variation of $\delta pH_b = pH_b - pH_{IEP} =$

$pH_b-(pK_+ + pK_-)/2$, Δ and salt concentration C_s on the insertion free energy curves and NP net charge profiles.

The general expressions for the free energy, eq 17, and for the NP charge, eq 21, in this case are simplified as

$$\Delta F_{ion}(z)/N_\Sigma k_B T = \frac{1}{2}\ln\left(\frac{10^{-\Delta}+10^{\Delta}+10^{-\delta pH_b}+10^{\delta pH_b}}{10^{-\Delta}+10^{\Delta}+10^{-\delta pH_b}\cdot\lambda^{-1}(z)+10^{\delta pH_b}\cdot\lambda(z)}\right) \tag{25}$$

$$Q(z)/N_\Sigma = \frac{1}{2}\left[\frac{10^{-\delta pH_b}\lambda^{-1}(z)-10^{\delta pH_b}\cdot\lambda(z)}{10^{\Delta}+10^{-\Delta}+10^{-\delta pH_b}\cdot\lambda^{-1}(z)+10^{\delta pH_b}\cdot\lambda(z)}\right] \tag{26}$$

By using eqs 24 and 25 one finds the height $\Delta F_{ion}(z^*)$ of the free energy barrier for the case of $f_+ = 0.5$ as

$$\Delta F_{ion}(z^*)/N_\Sigma k_B T = \frac{1}{2}\ln\left(\frac{10^{-\Delta}+10^{\Delta}+10^{-\delta pH_b}+10^{\delta pH_b}}{10^{-\Delta}+10^{\Delta}+2}\right) \tag{27}$$

As it follows from eqs 25, 26 and 27, at any given δpH_b the profiles of the free energy $\Delta F_{ion}(z)$ and particle net charge $Q(z)$ depend on the absolute value of Δ, but not on the sign of Δ, that is, coincide for the cases $pK_+ = pH_{IEP} \pm \Delta; pK_- = pH_{IEP} \mp \Delta$.

This feature is illustrated in **Figure 3** where $\Delta F_{ion}(z)$ and $Q(z)$ are plotted for several values of $\Delta pH_b = pH_b - pH_{IEP}$ and variable (symmetric) deviations $\pm\Delta$ of pK_+ and pK_- from common pH_{IEP}. In **Figure 3** the insertion free energy $\Delta F_{ion}(z)$ and the net charge of the NP $Q(z)$ are plotted at $pH_b > pH_{IEP}$ (left column) and $pH_b = pH_{IEP}$ (right column), by solid and dashed lines for cases $pK_+ < pK_-$ and $pK_+ > pK_-$, respectively. The $pK_+ = pK_-$ case is highlighted with a red dash - dot line. For each set of $\{pK_+, pK_-\}$, the isoelectric point is calculated according to the equation 12. Since $f_+ = 0.5$, the IEP for all the selected sets $\{pK_+, pK_-\}$ according to the eq 15 is $pH_{IEP} = 7$.

By setting $\Delta F_{ion}(z) = 0$ in eq 25, one finds that in the considered here case of $f_+ = 0.5$ the coordinate z_0 of vanishing of the free energy is independent of Δ and depends only on δpH_b, according to the following equation:

$$\psi(z_0) = -\frac{2\delta pH_b}{\log(e)} \tag{28}$$

i.e., at given δpH_b all the free energy curves corresponding to different Δ intersect in common point $z = z_0$ specified (for given parameters of the PE

Figure 3: Dependencies of the free energy $\Delta F_{ion}(z)$ (a) and net charge of the NP $Q(z)$ (b) on the distance from the grafting surface z, both normalized by N_Σ, for the cases above IEP ($\delta pH_b = 0.3 > 0$, left column) and at the IEP ($\delta pH_b = 0$, right column) at $f_+ = 0.5$ and $C_s = 0.001$. The color code corresponding to different set of symmetric ionization constants $pK_+ = pH_{IEP} \pm \Delta$ and $pK_- = pH_{IEP} \mp \Delta$, is indicated at the curves. The case of equal $pK_+ = pK_- = pH_{IEP}$ is highlighted by a red dash-dot curve. The brush parameters are: polymerization degree of the brush-forming chains $\mathcal{N} = 300$, reduced surface area per chain $S = s/a^2 = 100$, fraction of permanently (positively or negatively) charged monomer units $\beta = 0.5$. For all the curves $pH_{IEP} = (pK_+ + pK_-)/2 = 7$ (corresponding to eq 15). Arrows indicate the upper boundary of the brush ($z = H$).

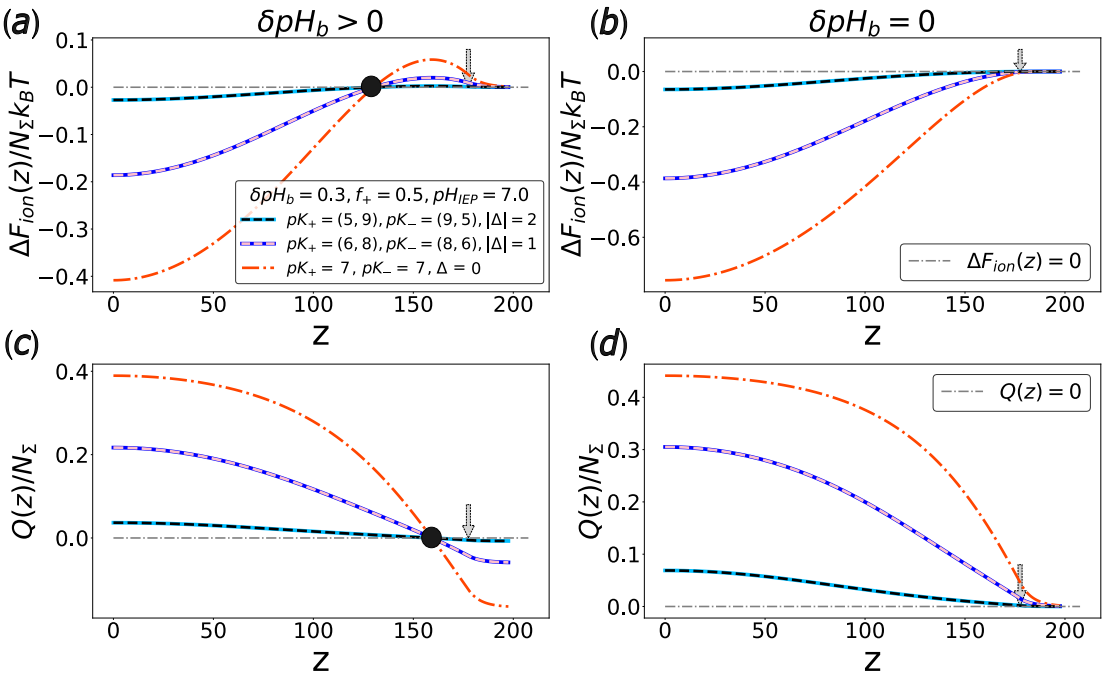

Figure 4: Dependencies of the NP charge inversion point z^* (green curve plotted according to eq 24) and the free energy vanishing point z_0 (orange curve, plotted according to eq 28 for the particular case of $f_+ = 0.5$). The parameters of the PE brush here and below are $\mathcal{N} = 300, S = s/a^2 = 100, a = l_B$ $C_s = 10^{-3}$.

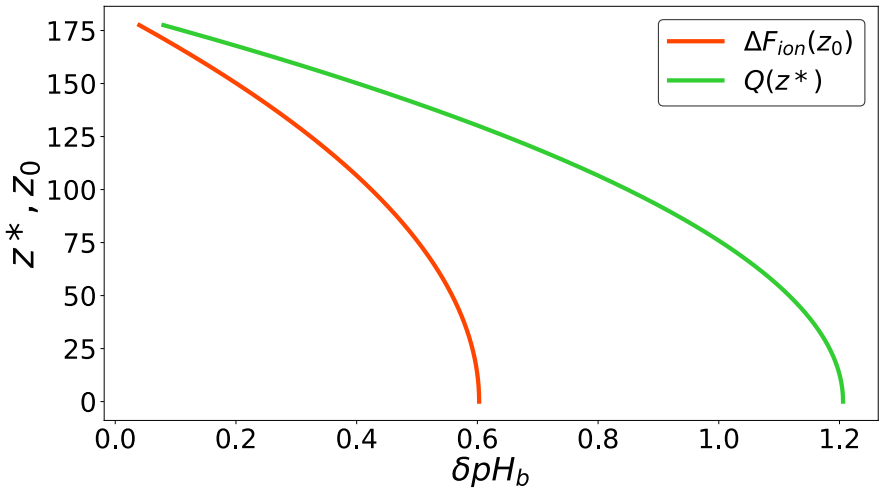

brush) by eq 28. The same refers to the $Q(z)$ profiles that intersect at $z = z^*$ given by eq 24.

The dependencies of the NP charge inversion coordinate z^* and coordinate z_0 of vanishing $\Delta F_{ion}(z)$ plotted as a function of δpH_b according to eqs 24 and 28, respectively, are presented in the **Figure 4**. As mentioned above, the $z^*(\delta pH_b)$ dependence is universal irrespectively of the NP parameters set $\{f_+, pK_+, pK_-\}$.

As can be seen from the **Figure 4**, both z^* and z_0 are monotonically decreasing function of the δpH_b, that is, the position z^* of the maximum in the $\Delta F_{ion}(z)$ curve and the coordinate z_0 of the free energy vanishing, $\Delta F_{ion}(z_0) = 0$ are displaced towards the grafting surface upon an increase in the deviation of pH_b from the IEP. Because $z_0 < z^*$, the $z_0(\delta pH_b)$ curve ends (that is, $z_0 = 0$) at some particular δpH_b value when $z^*(\delta pH_b)$ is still positive. At larger δpH_b the free energy $\Delta F_{ion}(z)$ is positive for $\forall z$, though exhibits a local edge minimum at $z = 0$ with $\Delta F_{ion}(z = 0) > 0$. This local minimum is separated from the bulk of the solution by the maximum at z^* and corresponds to the metastable state which disappears upon further increase in δpH_b when $z^* \to 0$. If δpH_b exceeds the value corresponding to vanishing z^*, the NP is negatively charged for $\forall z$, no charge inversion occurs.

By taking the derivative of the free energy given by eq 25 with respect to Δ and with the account of eq 28, one finds, that for any given coordinate z the free energy $\Delta F_{ion}(z)$ assumes the maximal and the minimal values at $\Delta = 0$, that is, for $pK_+ = pK_-$, if $z > z_0$ or $z < z_0$, respectively. This trend is also seen in **Figure 3**.

The **Figure 5** illustrates evolution of the free energy $\Delta F_{ion}(z)$ and charge $Q(z)$ profiles upon increasing deviation δpH_b from the common IEP $pH_{IEP} = (pK_+ + pK_-)/2 = 7$ for a set of $|\Delta| = (0; 1; 2)$. As discussed above and follows from eqs 25 and 26, the $\Delta F_{ion}(z)$ and $Q(z)$ profiles corresponding to $\pm\Delta$ superimpose.

At $\delta pH_b = 0.3$ and $\delta pH_b = 0.6$, the NP is negatively charged in the buffer, but the charge sign is changed to positive at $z = z^*$ upon the NP insertion into the brush. This charge inversion corresponds to the appearance of a maxima (potential barriers) in the $\Delta F_{ion}(z)$ curves. In the range of $z \leq z^*$ the free energy decreases upon approaching the grafting surface, passes through zero at $z = z_0$ and acquires a negative value at $z = 0$ that corresponds to thermodynamically favorable absorption of the NP by the brush.

For any given δpH_b the charge inversion point (the position of the maximum in the free energy) z^* , and the coordinate z_0 of vanishing free energy are independent of Δ, but both z^* and z_0 decrease upon increasing δpH_b, as follows from eqs 24 and 28. Importantly, for any given δpH_b, the magnitude of the maximum, $\Delta F_{ion}(z^*)$, and the depth of the edge minimum at the grafting surface, $|\Delta F_{ion}(z = 0)|$ decrease upon increasing $|\Delta|$; the same refers to the absolute values of the NP charge $|Q(z > z^*)|$ and $|Q(z < z^*)|$.

As the δpH_b increases (from 0.3 to 0.6 in the present case), for any given Δ, the height $\Delta F_{ion}(z^*)$ of the potential barrier increases and the depth of the pre-surface potential well $|\Delta F_{ion}(z = 0)|$ decreases. Hence, within certain range of the deviation of pH_b from the IEP, the NP absorption by the brush may remain thermodynamically favorable, but become kinetically hindered.

At even larger offset δpH_b from the IEP (e.g. at $\delta pH_b = 0.8$ in the present case), the free energy $\Delta F_{ion}(z)$ become positive, though a monotonically increasing function of z in the whole range of $0 \leq z \leq z^*$. That is, in the local edge minimum of $\Delta F_{ion}(z)$ reached at the grafting surface, $z = 0$, the free energy acquires a positive value. This minimum is still separated from the exterior region $z > z^*$ by the high potential barrier and corresponds to a metastable state of the NP in the brush. Remarkably, the height of the barrier $\Delta F_{ion}(z^*) - \Delta F_{ion}(z = 0)$ to be overcome by the particle to escape from the metastable state decreases and eventually vanish (when $z^* \to 0$) as δpH_b further increases: The NP is expelled from the brush.

The **Figure 6** illustrates evolution of the free energy $\Delta F_{ion}(z)$ and charge $Q(z)$ profiles upon increasing salt concentration plotted at fixed $\delta pH_b = 0.3$

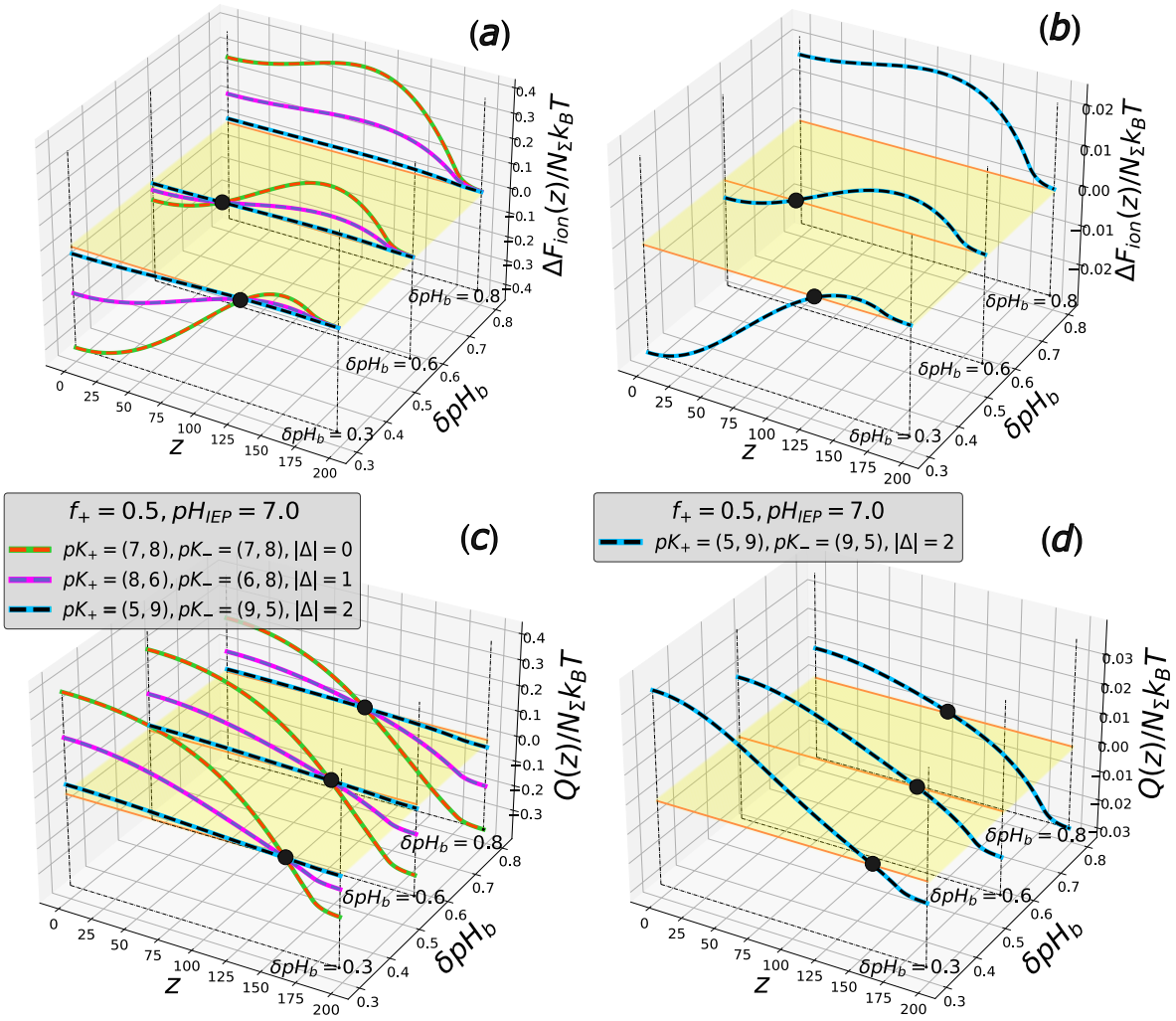

Figure 5: Cross-sections of the 2D profiles of the insertion free energy $\Delta F_{ion}(z, \delta pH_b)$ (a), (b) and NP charge $Q(z, \delta pH_b)$ (c), (d), both normalized by N_Σ, for the case of $f_+ = 0.5; (pK_+ + pK_-)/2 = pH_{IEP} = 7$ and varied $|\Delta| = |(pK_+ - pK_-)/2|$. Black circles in panels (a) and (b) correspond to the coordinate z_0 of vanishing of the free energy, black circles in the panels (c) and (d) correspond to the charge inversion points $z = z^*$.

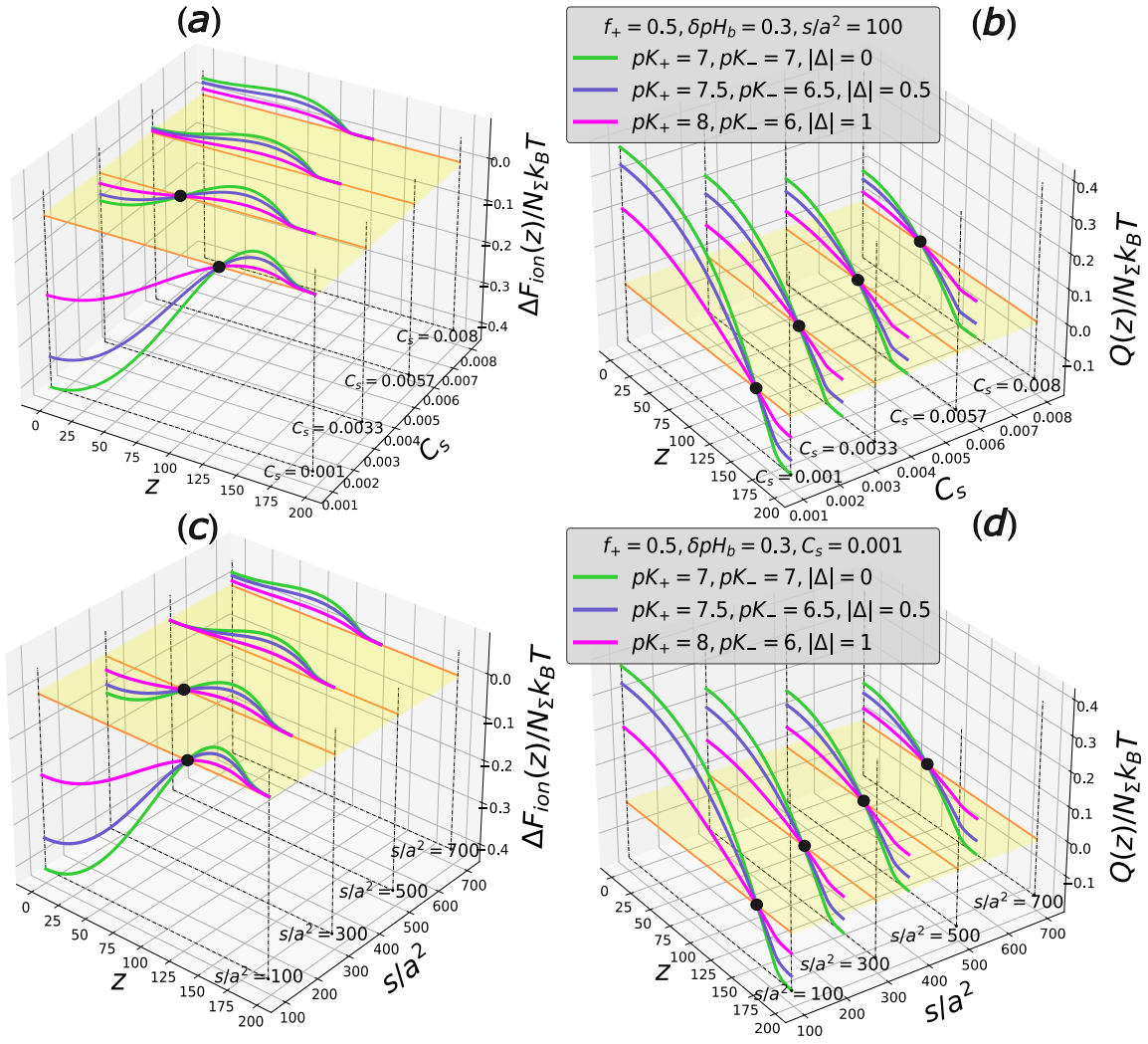

Figure 6: Cross sections of the 2D profiles of the insertion free energy $\Delta F_{ion}(z, C_s)$ (a), (c) and NP charge $Q(z, C_s)$ (b), (d), both normalized by N_Σ, for a set of values of pK_+, pK_- (with the corresponding color code). Black circles on the panels (a), (c) indicate points of vanishing free energy, $\Delta F_{ion}(z, C_s)$; black circles on the panels (b), (d) correspond to the charge inversion points $z = z^*$.

for three selected values of $|\Delta| = |(pK_+ - pK_-)/2|$. An increase in salt concentration leads to weakening of the electrical field created by PE brush, and the magnitude of the electrostatic potential decreases as it also show in **Figure 1c**. At low salt concentration, the NP is absorbed by the brush after overcoming the potential barrier. As it was shown earlier, for the case of equal $pK_+ = pK_-$, the potential barrier is maximal, and the depth of the pre-surface potential well is maximal as well.

As the salt concentration increases, the depth of the potential minimum decreases and the coordinates z_0 and z^* are shifted towards the grafting surface, because, as mentioned above, salt concentration affects the electrostatic potential profile $\psi(z) \equiv \ln \lambda(z)$. Note that the change in salt concentration does not affect the magnitude $\Delta F_{ion}(z^*)$ of the potential barrier because eq 27 does not contain $\lambda(z)$. Upon an increase in salt concentration, $z_0 \to 0$ and, at sufficiently high salt concentration the free energy remain positive for $\forall z \geq 0$. The persisting free energy edge minimum at $z = 0$ corresponds to a metastable state. Remarkably, the height of the barrier $\Delta F_{ion}(z^*) - \Delta F_{ion}(z = 0)$ to be overcome by the particle to escape from the metastable state decreases and eventually vanish (when $z^* \to 0$) as C_s further increases: The NP is expelled from the brush.

As shown in **Figure 6**, the free energy profiles evolve in a similar way upon variation of the grafting density, a^2/s, which as well as salt concentration, affects the shape of the brush electrostatic potential $\psi(z) \equiv \ln \lambda(z)$.

NP with varied proportion of cationic and anionic groups

As follows from eq 13 and illustrated by **Figure S1**, the isoelectric point depends on a set of parameters $pH_{IEP} = pH_{IEP}\ \{f_+, K_+, K_-\}$. Therefore, for a given value of pH_b and fixed $\{pK_+, pK_-\}$ the offset from the isoelectric point ($\delta pH_b = pH_b - pH_{IEP}$) depends on f_+.

In **Figure 7** the free energy $\Delta F_{ion}(z)$ and the NP charge $Q(z)$ are plotted for constant $pH_b = pK_+ = pK_-$ but varied f_+. As follows from eq 15, at $f_+ = 0.5$, pH_b coincides with pH_{IEP}, i.e. $\delta pH_b = 0$. At $f_+ \geq 0.5$, $\delta pH_b \leq 0$ which corresponds to a monotonically increasing free energy profile ($\Delta F_{ion}(z) \leq 0, (\partial \Delta F_{ion}(z)/\partial z > 0\ \forall z \in [0, \infty))$. In this case, the NP and the brush are oppositely charged, and the NP is driven into the brush by the attractive Coulomb force. On the contrary, at $f_+ \leq 0.5$, $\delta pH_b \geq 0$, the charge of the NP in the buffer is negative, $Q_b \leq 0$, but $Q(z)$ monotonically increases upon approaching the grafting surface and either remains negative $\forall z \in [0, \infty)$ or vanishes at $z = z^*$ and becomes positive for the NP located at $z < z^*$. Correspondingly, the free energy ΔF_{ion} is either positive and monotonously decreasing function $\forall z \in [0, \infty)$ (the NP expulsion

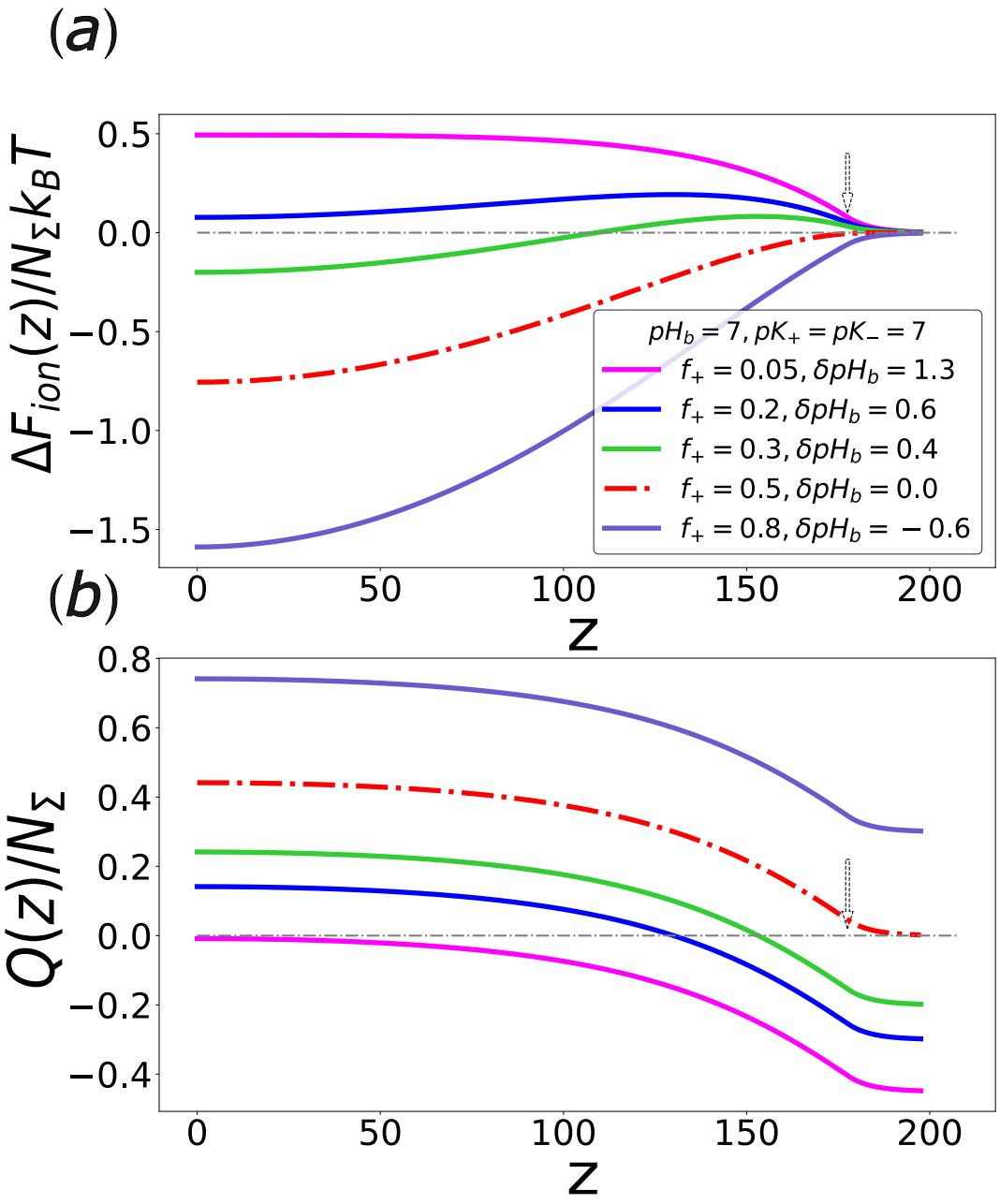

Figure 7: Position-dependent insertion free energy $\Delta F_{ion}(z)$ (a) and the NP charge $Q(z)$ (b) both normalized by N_Σ, as a function of the distance z from the grafting surface for a series of f_+ values at fixed pH_b. Arrows indicate the upper boundary of the brush. Dashed vertical lines indicate the charge inversion point, $z = z^*$. Dash-dot horizontal lines indicate $\Delta F_{ion}(z) = 0$ and $Q(z) = 0$.

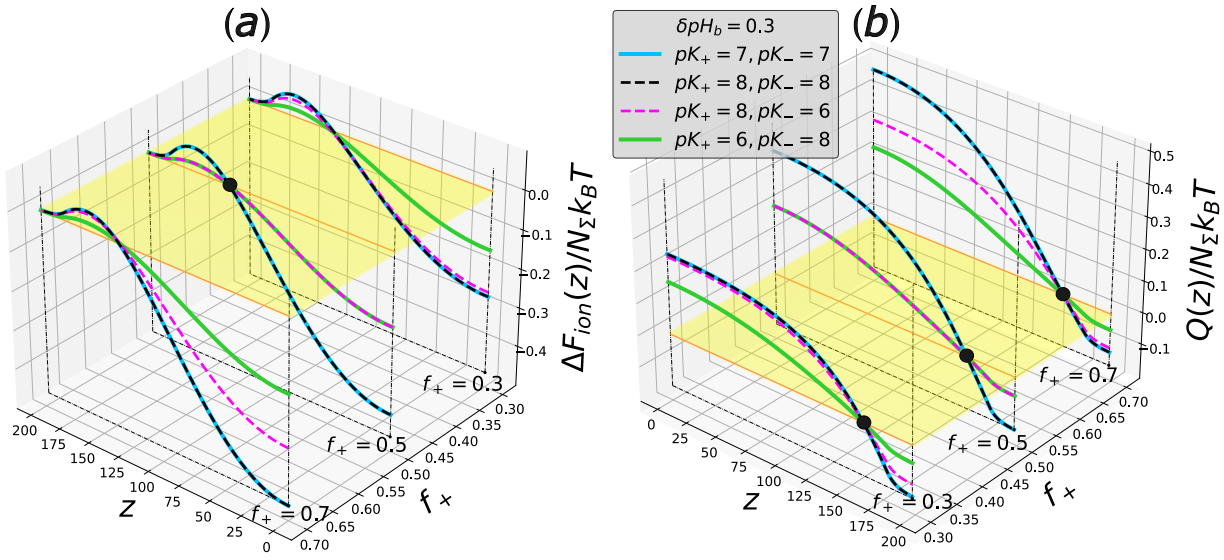

Figure 8: Cross sections of the 2D profiles of the insertion free energy $\Delta F_{ion}(z, f_+)$ (a) and NP charge $Q(z, f_+)$ (b), both normalized by N_Σ, for a set of values of $\{pK_+, pK_-\}$ (with the corresponding color code, as indicated at the curves). For all the curves $\delta pH(f_+, K_+, K_-) \equiv pH_b - pH_{IEP}(f_+, K_+, K_-) = 0.3$. Black circle in panel (a) indicate the coordinate $z = z_0$ of vanishing free energy, $\Delta F_{ion}(z_0, f_+) = 0$ at $f_+ = 0.5$; black circles in panel (b) correspond to the charge inversion points $z = z^*$ which are independent of f_+.

case) or exhibits a maximum at $z = z^*$ and becomes an increasing function of z in the range of $0 \leq z \leq z^*$. As the fraction f_+ of cationic groups on the particle surface decreases, the magnitude of the charge $Q(z = 0)$ and the depth $|\Delta F_{ion}(z = 0)|$ of the free energy edge minimum at the grafting surface decrease. In the latter case the NP absorption of the brush is thermodynamically favorable as long as $\Delta F_{ion}(z = 0) < 0$, or the NP can be kinetically entrapped inside the brush in local free energy minimum with $\Delta F_{ion}(z = 0) > 0$, which corresponds to a metastable state.

In **Figure 8 a,b** we show cross sections of 2D profiles of the insertion free energy $\Delta F_{ion}(z, f_+)$ and net charge $Q(z, f_+)$ of the NP plotted at four selected values of $\{pK_+, pK_-\}$. All cross sections are plotted for the case $pH_b > pH_{IEP}$, i.e. for each set of $\{f_+, pK_+, pK_-\}$ the isoelectric point $pH_{IEP}\{f_+, pK_+, pK_-\}$ is calculated and an equal offset ($\delta pH_b = 0.3$) is made from it. In the considered here case $\delta pH_b > 0$, the NP is negatively charged in the solution, but changes the sign of the charge to the opposite upon entering the brush. The change of the charge sign corresponds to the appearance

of a potential barrier on the re-ionization free energy curve. Because for all the curves $\delta pH_b = const$, all the $Q(z)$ curves in **Figure 8 b** pass through zero at the same point $z = z^*$, according to eq 24. The free energy curves $\Delta F_{ion}(z)$ corresponding to different sets of $\{pK_+, pK_-\}$ vanish at the same coordinate $z = z_0$ only at $f_+ = 0.5$, according to eq 28, whereas at $f_+ \neq 0.5$ the $\Delta F_{ion}(z)$ curves corresponding to different sets of $\{pK_+, pK_-\}$ vanish at different points $z = z_0\{f_+, pK_+, pK_-\}$.

Remarkably, at $pK_+ = pK_- = pK^{(m)}$ the $\Delta F_{ion}(z)$ and $Q(z)$ curves superimpose irrespectively of the $pK^{(m)}$ value at any chosen value of f_+. This superposition follows directly from eqs 17 and 21 that can be presented as

$$\Delta F_{ion}(z)/N_\Sigma k_B T = f_+ \ln\left(\frac{\lambda(z)\cdot(1+10^{\delta pH_b+pH_{IEP}-pK_+})}{1+10^{\delta pH_b+pH_{IEP}-pK_+}\cdot\lambda(z)}\right)+(1-f_+)\ln\left(\frac{\lambda^{-1}(z)\cdot(1+10^{pK_--\delta pH_b-pH_{IEP}})}{1+10^{pK_--\delta pH_b-pH_{IEP}}\cdot\lambda^{-1}(z)}\right) \quad (29)$$

$$\frac{Q(z)}{k_B T N_\Sigma} = \frac{f_+}{1+10^{\delta pH_b+pH_{IEP}-pK_+}\cdot\lambda(z)} - \frac{(1-f_+)}{1+10^{pK_--\delta pH_b-pH_{IEP}}\cdot\lambda^{-1}(z)} \quad (30)$$

with $pK_+ = pK_- = pK^{(m)}$ and from eq 14, follows that $pH_{IEP} - pK^{(m)} = \log(f_+/(1-f_+))$.

By combining eqs 29 and 24 one finds also the height of the maximum of the free energy in the charge inversion point z^* as

$$\Delta F_{ion}(z^*)/N_\Sigma k_B T = f_+ \ln\left(\frac{10^{-\delta pH_b}+10^{pH_{IEP}-pK_+}}{1+10^{pH_{IEP}-pK_+}}\right)+(1-f_+)\ln\left(\frac{10^{\delta pH_b}+10^{pK_--pH_{IEP}}}{1+10^{pK_--\delta pH_b-pH_{IEP}}}\right) \quad (31)$$

which is controlled only by the NP properties and pH_b, but is independent of the brush parameters (i.e., independent of $\lambda(z)$).

The **Figure 8 a,b** also shows that even in the case of $f_+ \neq 0.5$ the height of the potential barrier at $z = z^*$ and the depth of the potential minimum at $z = 0$ in the free energy curves are greater at $pK_+ = pK_- = pK^{(m)}$ than for the case of unequal ionization constants, i.e., $(pK_+ + pK_-)/2 = pK^{(m)}$, $pK_+ - pK_- \neq 0$. Similarly, the negative charge of the NP, with equal $pK_+ = pK_- = pK^{(m)}$, in the buffer is larger in the absolute value, but as it approaches the grafting surface, it becomes more positively charged. In other words, the amplitude of the variation of the NP charge and free

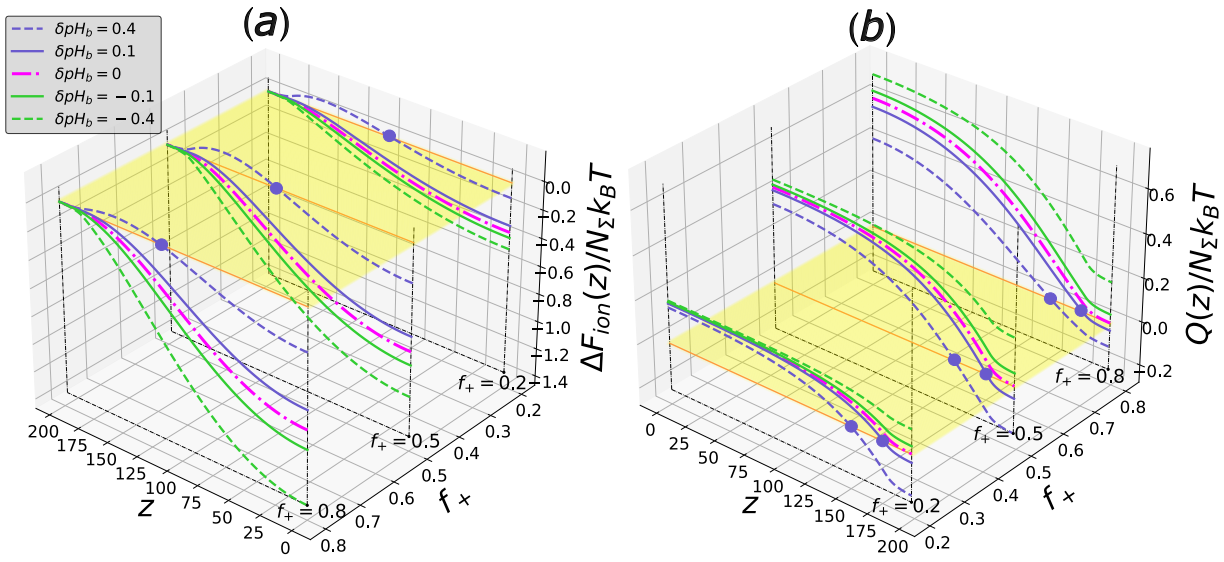

Figure 9: Cross sections of the 2D profiles of the insertion free energy $\Delta F_{ion}(z, f_+)$ (a) and NP charge $Q(z, f_+)$ (b), both normalized by N_Σ, for a set of values of $\delta pH_b \in [-0.4; 0.4]$ (with the corresponding color code, as indicated at the curves). All cross sections are plotted for the case $f_+ = 0.5$ and $pK_+ = pK_- = pK^{(m)} = 7$. Violet circles in panel (a) indicate points $z = z_0$ of vanishing free energy, $\Delta F_{ion}(z_0, f_+) = 0$; violet circles in panel (b) correspond to the charge inversion points $z = z^*$.

energy is greater for the case of $pK_+ = pK_- = pK^{(m)}$, than in the case $(pK_+ + pK_-)/2 = pK^{(m)}, pK_+ - pK_- \neq 0$. It can also be noted that for the case of $f_+ = 0.5$, the potential barrier on the ionization free energy curve is higher than for $f_+ \neq 0.5$. As it is also shown in **Figure 8 a,b**, that the curves of the free energy and the charge are superimposed for $(pK_+ + pK_-)/2 = pK^{(m)}, pK_+ - pK_- = \pm 2\Delta$ only at $f_+ = 0.5$, whereas upon deviation from $f_+ = 0.5$, the free energy and charge curves diverge.

In **Figure 9 a,b** we show cross sections of 2D profiles of the insertion free energy $\Delta F_{ion}(z, f_+)$ and net charge $Q(z, f_+)$ of the NP plotted at selected values of $\delta pH_b \in [-0.4; 0.4]$ for the case $pK_+ = pK_- = pK^{(m)} = 7$. In the region $\delta pH_b < 0$, the NP in the solution is positively charged and remains positively charged throughout the entire thickness of the brush, with the charge increasing in absolute value as the NP approaches the grafting surface of the brush. This corresponds to a monotonically increasing as a function of z re-ionization free energy profile. As the δpH_b increases (when passing through an isoelectric point $\delta pH_b = 0$), the NP in the solution acquires a negative charge, but when the NP enters the brush, the sign of the charge is

changed to the opposite. This corresponds to the appearance of a potential barrier on the re-ionization free energy curve. For any given δpH_b the height of the potential barrier is the largest at $f_+ = 0.5$, as also shown in **Figure 8 a**. **Figure 9** also demonstrates that with an increase in the fraction f_+ of cationic groups on the NP surface, the amplitude of the change in free energy and the NP charge upon moving from the buffer into the brush increases.

In **Figure 10 a,b** we show 2D profiles of the insertion free energy $\Delta F_{ion}(z, \delta pH_b, f_+ = 0.5)$ (a), $\Delta F_{ion}(z, f_+, \delta pH_b = 0.4)$ (c) and net charge $Q(z, \delta pH_b, f_+ = 0.5)$ (b), $Q(z, f_+, \delta pH_b = 0.4)$ (d) of the NP plotted at three selected values of $pK_+ = pK_- = pK^{(m)} = (5; 7; 9)$. As follows from **Figure 10**, the free energy and the charge dependencies on z, f_+ at constant δpH_b or on $z, \delta pH_b$ at constant f_+ plotted for different values of $pK^{(m)}$ superimpose, as it follows from eq 14 and eqs 29 and 30.

Conclusions

Electrostatic interactions between ampholytic nanoparticles (with globular proteins among them) and polyelectrolyte brushes are controlled by few sets of parameters: Environmental conditions (buffer pH and salt concentration), brush architecture (degree of polymerization and fraction of charged monomer units in the brush-forming chains, the grafting density), and composition of cationic and anionic groups (amino acid residues) on the NP surface and their ionization constants are among them. Deviations in pH_b from the IEP that control the net charge of NP in buffer solution, have the strongest effect: The NP is attracted to or repelled by the PE brush in the cases when it is charged oppositely or similarly to the brush, respectively. However, because of the shift in local pH inside the brush with respect to its buffer value, pH_b, the net charge of the NP may invert its sign upon NP insertion into a similarly charged brush. This finding is in a line with results of numerical calculations based on the Scheutjens-Fleer self-consistent field numerical method.[64] In such cases the NP may overcome the repulsive potential barrier at the periphery of the brush, change the charge sign, and be further driven into the brush by the electrostatic forces. Then depending on whether the NP free energy inside the brush is negative or positive (with respect to the reference state in the buffer) the NPs are either spontaneously absorbed and accumulated inside the brush, or eventually expelled from the brush: In the latter case localization of the NP in the brush corresponds to a metastable state. The depth of the free energy minimum inside the brush is amplified as the ionic strength in the solution diminishes whereas the height

Figure 10: 2D profiles of the insertion free energy $\Delta F_{ion}(z, \delta pH_b, f_+ = 0.5)$ (a), $F_{ion}(z, f_+, \delta pH_b = 0.4)$ (c) and NP charge $Q(z, \delta pH_b, f_+ = 0.5)$ (b), $Q(z, f_+, \delta pH_b = 0.4)$ (d), all are normalized by N_Σ, for a set of values of $pK_+ = pK_- = pK^{(m)} = (5; 7; 9)$ (with the corresponding color code, as indicated at the curves).

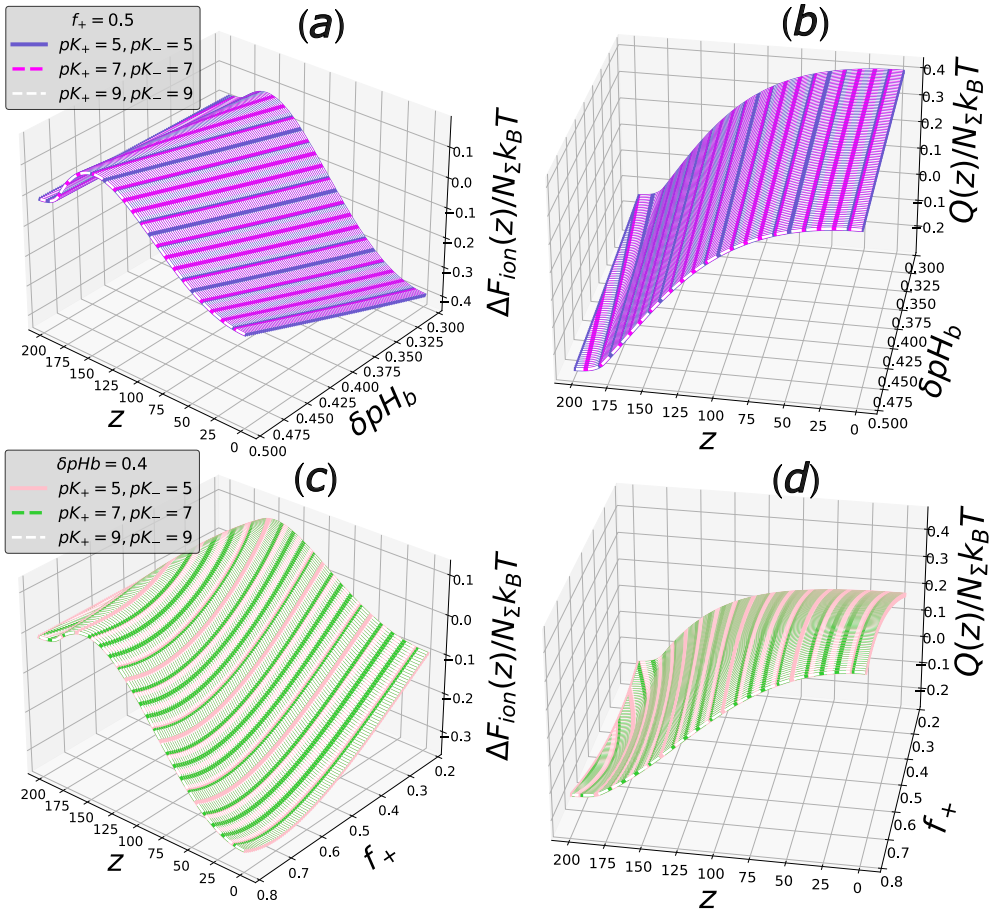

of the potential barrier is insensitive to salt concentration. Therefore, the NP absorption by the brush is suppressed thermodynamically or kinetically hindered at high ionic strength.

As discussed above, the NPs comprising different sets of cationic and anionic groups with their respective ionization constants may have the same IEP, i.e., their net charge vanish at the same buffer pH_b. As we have demonstrated in this study, the deviation of the pH_b from the pH_{IEP} (at fixed salt concentration and brush parameters) does not uniquely control the electrostatic part of the NP insertion free energy $\Delta F_{ion}(z)$ and the NP position-dependent net charge $Q(z)$ and thus the absorption/depletion scenario. Both the depth of the free energy minimum inside the brush and the height of the potential barrier depend also on the values of ionization constants of cationic and anionic groups.

We have examined this effect using a simplified though realistic model of the NP comprising one type of cationic and one type of anionic groups in equal proportion. We expect, however, that general trends remain the same if the NP comprises in approximately equal proportion a few types of cationic and anionic groups with close values of the (acidic) ionization constants.

We have found, that for any given deviation $\delta pH_b > 0$ from the IEP, the absolute values of the NP negative charge in the buffer and positive charge in the brush decrease as the absolute value of the difference $|2\Delta| \equiv |pK_+ - pK_-|$ increases. The same refers to the height of the potential barrier and the depth of the free energy edge minimum reached at the grafting surface. Remarkably, the free energy and the charge profiles superimpose in the cases of $pK_+ - pK_- = \pm 2\Delta$. The positions of the maximum in the free energy, as well as common coordinate corresponding to vanishing of the position-dependent free energy depend only on the offset δpH_b from the IEP, but are independent of the difference $2|\Delta|$ between the values of the ionization constants.

Hence, the NP charge inversion upon insertion into the similarly charged brush is most pronounced in the case of (approximately) equal ionization constants, that leads also to the deepest free energy minimum inside the brush. Therefore, one can conclude that for given offset $\delta pH_b \geq 0$ from the IEP an uptake of NP by similarly (negatively) charged brush is thermodynamically most favorable in the case of (approximately) equal acidic ionization constants of cationic and anionic groups. At the same time, however, the height of the free energy barrier to be overcome by the NP to penetrate the brush is also the largest for the case of equal ionization constants. Remarkably, the value of the free energy $\Delta F_{ion}(z = 0)$ can be tuned (from negative to positive) at constant $\delta pH_b \geq 0$ by increasing salt concentration, whereas the height of the potential barrier is virtually independent of the ionic strength.

The presented above theoretical consideration can be easily extended for the case of polycationic (positively charged) brush. In particular, the insertion free energy profile $\Delta F_{ion}(z)$, eq 25, and the height of the potential barrier, $\Delta F_{ion}(z^*)$, eq 27, remain invariant upon replacing $\lambda(z) \rightarrow \lambda^{-1}(z)$ and $\delta pH_b \rightarrow -\delta pH_b$, whereas the NP net charge profile $Q(z)$, eq 26, only changes the sign.

The impact of various parameters on protein absorption by brushes on the "wrong" side of the isoelectric point (IEP) has been amply investigated experimentally . These parameters include protein type,[57–59] salt concentration,[50,56,59,60] and pH of the solution.[57,61,62] Alexander Wittemann and Matthias Ballauff et al.[55,58] studied protein absorption on polyanionic brushes, with a focus on protein type and salt concentration. The proteins analyzed were bovine serum albumin (BSA), β-lactoglobulin (BLG), and bovine pancreatic ribonuclease A (RNase A), absorbed on spherical polyelectrolyte brushes. These brushes consisted of poly(styrene) core with grafted linear chains of strong, poly(styrenesulfonate) (PSS), or weak, poly(acrylic acid) (PAA) anionic polyelectrolytes. The results revealed that both BSA and β-lactoglobulin were strongly absorbed on the "wrong" side of the isoelectric point (at $pH = 6.1$) by both strong and weak polyanionic brushes at low salt concentrations. However, as the salt concentration increased, a significant fraction of protein was repelled out of the brushes. Furthermore, it was observed that β-lactoglobulin had a lower capability compared to BSA, which could be attributed to the smaller fraction of cationic groups on the surface of β-lactoglobulin. It was also found that the ability to bind proteins was higher for PSS compared to PAA brushes, likely due to the lower pH in strong polyelectrolyte brush. It was found that that BSA exhibited strong adsorption on SPB as long as the ionic strength remained low.[55] Wang et al.[61] studied adsorption of proteins, BSA and BLG, on spherical cationic and anionic polyelectrolyte brushes. The polyelectrolyte brushes consisted of linear chains of weak polyelectrolytes, either anionic PAA or cationic poly(2-aminoethyl methacrylate hydrochloride) (PAEMH), grafted onto polystyrene core particles. It was shown that the protein absorption by the brush is strongly influenced by the pH of the solution. Both PAA and PAEMH brushes absorb proteins slightly above/below the protein IEP, whereas at pH significantly higher/lower than the IEP no protein absorption was observed.

The observed in refs[55,58,61] dependencies of the protein absorption on pH and ionic strength of the solution fully agree with predictions of our mean-field theory. Additionally, it was found in ref[61] that the type of protein influenced its absorption behavior. It was found, BSA exhibited better absorption on an anionic brush compared to BLG, whereas BLG showed better

absorption on a cationic brush. According to our theory, this difference can be explained by different proportions of cationic and anionic groups present on the proteins surface.

The NP re-ionization leading to appearance of the thermodynamic driving force for the NP uptake by the brush is most pronounced at low salt concentration, typical for artificial (e.g, protein separation) systems. Addition of salt to the solution leads to pronounced decrease in the magnitude of the electrostatic potential inside the brush (Figure 1c) and thus to weakening of the re-ionization of the NP inside the brush. As a result, the depth of the attractive minimum in the free energy inside the brush decreases, whereas the height of the potential barrier is unaffected by salt at constant $(pH_b - pH_{IEP})$. Under physiological conditions (corresponding to reduced salt concentration C_s on the order of 10^{-2} in our units) the free energy minimum with a negative value exists only at pH_b sufficiently close to the IEP (about $\delta pH_b = 0.1$). However, the range of $(pH_b - pH_{IEP})$ where the NP re-ionization is significant can be extended if the NP interacts with a brush with higher grafting or charge density (cf Figure 1b). In biological systems re-ionization may occur for proteins interacting with pericellular layers of strongly charged GAGs. The value of Δ for typical amino acid residues in proteins is about 2. As follows, e.g., from Figure 3, this leads to a decrease in the depth of the proximal free energy minimum by the order of magnitude. However, the absolute value of the free energy in the minimum (multiplied by $N_{Sigma} \sim 10^2$) may be still on the order of a few k_BT which is sufficient for accumulation of the NPs in the brush. At the same time, an increase in Δ leads to a concomitant decrease in the height of the potential barrier that promotes absorption.

We recall that apart from the considered here electrostatic contribution $\Delta F_{ion}(z)$, the net insertion free energy comprises also repulsive osmotic term proportional to the NP volume and short-range non-electrostatic (e.g., hydrophobic) interactions that do not depend on pH_b and on the composition of cationic and anionic groups on the NP surface, but depend on salt concentration and thus contribute to the overall free energy balance.

To summarize, the developed theory unravels on the mean-field level the mechanism of the NP/protein interactions with polyelectrolyte brush and correctly captures experimentally established trend of suppression of the NP/protein absorption by the brush upon an increase in salt concentration or/and pH offset on the "wrong side" of the IEP. It is also demonstrated that the larger is the difference between pK values for cationic and anionic groups on the particle surface, the weaker is thermodynamic driving force for the absorption. The theory has also led to two non-trivial predictions: (i) Existence of metastable states of the protein/NP with reversed charge inside

the brush which implies that charge reversal is necessary, but insufficient condition for equilibrium absorption of NPs in the brush; (ii) Kinetic rather than thermodynamic control of the protein absorption by similarly charged brush due to the free energy barrier at the periphery of the brush; the height of the barrier increases as a function of the pH offset from the IEP, but is fairly independent of salt concentration and brush properties at given pH. These theoretical results can be used for quantitative predicting interaction patterns of polyelectrolyte brushes with globular proteins and ampholytic nanocolloids with low asymmetry in surface charge distribution.

Supporting information

Plots of electrostatic potential in the polyanionic brush in the proximal to the grafting surface region, plots of the isoelectric point dependence on fraction f_+ of cationic groups for different sets of ionization constants, 2D plots of the isoelectric point on ionization constants of cationic and anionic groups at their varied proportion.

Acknowledgments

This work was supported by the Russian Science Foundation, grant 23-13-00174

References

[1] Klein, J.; Kumacheva, E.; Mahalu, D.; Perahia, D.; Fetters, L. J. Reduction of frictional forces between solid surfaces bearing polymer brushes. *Nature* **1994**, *370(6491)*, 634-636.

[2] Schorr, P. A.; Kwan, T. C.; Kilbey, S. M.; Shaqfeh, E. S.; Tirrell, M. Shear forces between tethered polymer chains as a function of compression, sliding velocity, and solvent quality. *Macromolecules* **2003**, *36(2)*, 389-398.

[3] Lee, S.; Spencer, N. D. Sweet, hairy, soft, and slippery. *Science* **2008**, *319(5863)*, 575-576.

[4] Chen, M.; Briscoe, W. H.; Armes, S. P.; Klein, J. Lubrication at physiological pressures by polyzwitterionic brushes. *Science* **2009**, *323(5922)*, 1698-1701.

[5] Zhulina, E. B.; Rubinstein, M. Lubrication by polyelectrolyte brushes. *Macromolecules* **2014**, *47(16)*, 5825-5838.

[6] Napper, D. H. *Polymeric stabilization of colloidal dispersions*; Academic Press: New York, 1983.

[7] Israelachvili, J.N. *Intermolecular and Surface Forces: With Applications to Colloidal and Biological Systems*; Academic Press: New York, 1985

[8] Pincus, P.A. Colloid stabilization with grafted polyelectrolytes. *Macromolecules* **1991**, *24(10)*, 2912-2919.

[9] Weir, M. P.; Heriot, S. Y.; Martin, S. J.; Parnell, A. J.; Holt, S. A.; Webster, J. R.; Jones, R. A. Voltage-induced swelling and deswelling of weak polybase brushes. *Langmuir* **2011**, *27(17)*, 11000-11007.

[10] Drummond, C. Electric-field-induced friction reduction and control. *Phys. Rev. Lett.* **2012**, *109(15)*, 154302.

[11] Sénéchal, V.; Saadaoui, H.; Rodriguez-Hernandez, J.; Drummond, C. Electrowetting of weak polyelectrolyte-coated surfaces. *Langmuir* **2017**, *33(20)*, 4996-5005.

[12] Borisova, O. V.; Billon, L.; Richter, R. P.; Reimhult, E.; Borisov, O. V. pH-and Electro-Responsive Properties of Poly (acrylic acid) and Poly

(acrylic acid)-block-poly (acrylic acid-grad-styrene) Brushes Studied by Quartz Crystal Microbalance with Dissipation Monitoring. *Langmuir* **2015**, *31(27)*, 7684-7694.

[13] Kabanov, A.V.; Kabanov, V.A. Interpolyelectrolyte and block ionomer complexes for gene delivery: physico-chemical aspects. *Adv. Drug Deliv. Rev.* **1998**, *30(1-3)*, 49-60.

[14] Schallon, A.; Synatschke, C. V.; Jérôme, V.; Müller, A. H. E.; Freitag, R. Nanoparticulate nonviral agent for the effective delivery of pDNA and siRNA to differentiated cells and primary human T lymphocytes. *Biomacromolecules* **2012**, *13(11)*, 3463-3474.

[15] Miyata, K.; Nishiyama, N.; Kataoka, K. Rational design of smart supramolecular assemblies for gene delivery: chemical challenges in the creation of artificial viruses. *Chem. Soc. Rev.* **2012**, *41(7)*, 2562-2574.

[16] Yu, T.;, Liu, X.; Bolcato-Bellemin, A.-L.; Wang, Y.; Liu, C.; Erbacher, P.; Qu, F.; Rocchi, P.; Behr, J.-P.; Peng, L. An amphiphilic dendrimer for effective delivery of small interfering RNA and gene silencing in vitro and in vivo. *Angew. Chem. Int. Ed.* **2012**, *51(34)*, 8478-8484.

[17] Liu, X.; Zhou, J.; Yu, T.; Chen, C.; Cheng, Q,; Sengupta, K.; Huang, Y.; Li, H.; Liu, C.; Wang, Y.; Pososso, P.; Wang, M.; Cui, Q.; Giorgio, S.; Fermeglia, M.; Qu, F.; Pricl, S.; Shi, Y.; Liang, Z.; Rocchi, P.; Rossi, J.J.; Peng, L. Adaptive amphiphilic dendrimer-based nanoassemblies as robust and versatile siRNA delivery systems. *Angew. Chem. Int. Ed.* **2014**, *53(44)*, 11822-11827.

[18] Fan, X., Zhao, Y., Xu, W., Li, L. . Linear–dendritic block copolymer for drug and gene delivery. *Mater. Sci. Eng. C* **2016**, *62*, 943-959.

[19] Bysell, H.; Mansson, R.; Hansson, P.; Malmsten, M. Microgels and microcapsules in peptide and protein drug delivery. *Adv. Drug Deliv. Rev.* **2011**, *63(13)*, 1172-1185.

[20] Braatz, D.; Dimde, M.; Ma, G.; Zhong, Y.; Tully, M.; Grotzinger, C.; Zhang, Y.; Mavroskoufis, A.; Schirner, M.; Zhong, Z.; Ballauff, M.; Haag, R., Toolbox of Biodegradable Dendritic (Poly glycerol sulfate)–SS-poly (ester) Micelles for Cancer Treatment: Stability, Drug Release, and Tumor Targeting. *Biomacromolecules* **2021**, *22(6)*, 2625-2640.

[21] Kiani, C.; Chen, L.; Wu, Y. J.; Yee, A. J.; Yang, B. B. Structure and functions of aggrecan. *Cell Res.* **2002**, *12*, 19-32.

[22] Achazi, K.; Haag, R.; Ballauff, M.; Dernedde, J.; Kizhakkedathu, J. N.; Maysinger, D.; Multhaup, G. Understanding the interactions of polyelectrolyte architectures with proteins and biosystems. *Angew. Chem. Int. Ed.* **2021**, *60(8)*, 3882-3904.

[23] Nie, C. A. X.; Pouyan, P.; Lauster, D.; Trimpert, J.; Kerkhoff, Y.; Szekeres, G. P.; Wallert, M.; Block, S.; Sahoo, A. K.; Dernedde, J.; Pagel, K.; Kaufer, B. B.; Netz, R. R.; Ballauff, M.; Haag, R. Polysulfates Block SARS-CoV-2 Uptake through Electrostatic Interactions. *Angew. Chem. Int. Ed.* **2021**, *60(29)*, 15870-15878.

[24] Kapelner, R. A.; Yeong, V.; Obermeyer, A. C. Molecular determinants of protein-based coacervates. *Current Opin. Colloid Interface Sci.* **2021**, *52*, 101407.

[25] Yeong, V.; Werth, E. G.; Brown, L. M.; Obermeyer, A. C. Formation of biomolecular condensates in bacteria by tuning protein electrostatics. *ACS Cent. Sci.* **2020**, *6(12)*, 2301-2310.

[26] Cagno, V.; Tseligka, E. D.; Jones, S. T.; Tapparel, C. Heparan sulfate proteoglycans and viral attachment: true receptors or adaptation bias? *Viruses* **2019**, *11(7)*, 596.

[27] Borisov, O. V.; Birshtein, T. M.; Zhulina, E. B. Collapse of grafted polyelectrolyte layer. *J. Phys. II* **1991**, *1(5)*, 521-526

[28] Wittmer J.; Joanny J. F. Charged diblock copolymers at interfaces. *Macromolecules* **1993**, *26(11)*, 2691-2697.

[29] Borisov, O. V.; Zhulina, E. B.; Birshtein, T. M. Diagram of the states of a grafted polyelectrolyte layer. *Macromolecules* **1994**, *27(17)*, 4795-4803.

[30] Zhulina, E.B.; Birshtein, T.M.; Borisov, O.V. Theory of ionizable polymer brushes. *Macromolecules* **1995**, *28(5)*, 1491-1499.

[31] Guenoun, P.; Schalchli, A.; Sentenac, D.; Mays, J. W.; Benattar, J. J. Free-standing black films of polymers: a model of charged brushes in interaction. *Phys. Rev. Lett.* **1995**, *74(18)*, 3628.

[32] Mir, Y.; Auroy, P.; Auvray, L. Density profile of polyelectrolyte brushes. *Phys. Rev. Lett.* **1995**, *75(15)*, 2863.

[33] Ahrens, H.; Förster, S.; Helm, C.A. Charged polymer brushes: counterion incorporation and scaling relations. *Phys. Rev. Lett.* **1998**, *81(19)*, 4172.

[34] Currie, E. P. K.; Sieval, A. B.; Fleer, G. J.; Stuart, M. C. Polyacrylic acid brushes: surface pressure and salt-induced swelling. *Langmuir* **2000**, *16(22)*, 8324-8333.

[35] Wesley, R. D.; Cosgrove, T.; Thompson, L.; Armes, S. P.; Billingham, N. C.; Baines, F. L. Hydrodynamic layer thickness of a polybase brush in the presence of salt. *Langmuir* **2000**, *16(10)*, 4467-4469.

[36] Konradi, R.; Rühe, J. Interaction of poly (methacrylic acid) brushes with metal ions: Swelling properties. *Macromolecules* **2005**, *38(10)*, 4345-4354.

[37] J. Rühe, M.; Ballauff, M.; Biesalski, P.; Dziezok, F.; Gröhn, D.; Johannsmann, N.; Houbenov, N.; Hugenberg, R.; Konradi, S.; Minko, M.; Motornov, R. R.; Netz, M.; Schmidt, C.; Seidel, M.; Stamm, T.; Stephan, D.; Usov, H.; Zhan, H. Polyelectrolyte Brushes. *Adv. Polym. Sci.* **2004**, 165, 79-150.

[38] Ballauff, M.; Borisov, O.V. Polyelectrolyte brushes. *Curr. Opin. Colloid Interface Sci.* **2006**, *11(6)*, 316-323.

[39] Toomey, R.; Tirrell, M. Functional polymer brushes in aqueous media from self-assembled and surface-initiated polymers. *Annu. Rev. Phys. Chem.* **2008**, *59*, 493-517.

[40] Zhulina, E.B.; Borisov, O.V. Structure and interaction of weakly charged polyelectrolyte brushes: Self-consistent field theory. *J. Chem. Phys.* **1997**, *107(15)*, 5952-5967.

[41] Zhulina, E.B.; Klein Wolterink, J.; Borisov, O.V. Screening effects in a polyelectrolyte brush: Self-consistent-field theory. *Macromolecules* **2000**, *33(13)*, 4945-4953.

[42] Lebedeva I.O.; Zhulina E.B.; Borisov O.V. Self-consistent field theory of polyelectrolyte brushes with finite chain extensibility. *J. Chem. Phys.* **2017**, *146(21)*, 214901.

[43] Zhulina, E. B.; Borisov, O. V. Poisson–Boltzmann theory of pH-sensitive (annealing) polyelectrolyte brush. *Langmuir* **2011**, *27(17)*, 10615-10633.

[44] Zhulina, E. B.; Boulakh, A. B.; Borisov, O. V. Repulsive forces between spherical polyelectrolyte brushes in salt-free solution. *Z. Phys. Chem.* **2012**, *226(7-8)*, 625-643.

[45] Zhulina E. B., Borisov O. V. Brushes of dendritically branched polyelectrolytes. *Macromolecules* **2015**, *48(5)*, 1499-1508.

[46] Zhulina, E. B.; Rubinstein, M. Ionic strength dependence of polyelectrolyte brush thickness. *Soft matter* **2012**, *8(36)*, 9376-9383.

[47] Ye, Z.; Li, L.; Dai, L.; Wang, Y.; Yang, Q.; von Klitzing, R.; Guo, X. Selective uptake of different proteins by annealed and quenched cationic spherical polyelectrolyte brushes. *J. Polym. Sci.* **2020**, *58(21)*, 3018-3030.

[48] Henzler, K.; Wittemann, A.; Breininger, E.; Ballauff, M.; Rosenfeldt, S. Adsorption of bovine hemoglobin onto spherical polyelectrolyte brushes monitored by small-angle X-ray scattering and Fourier transform infrared spectroscopy. *Biomacromolecules* **2007**, *8(11)*, 3674-3681.

[49] Rosenfeldt, S.; Wittemann, A.; Ballauff, M.; Breininger, E.; Bolze, J.; Dingenouts, N. Interaction of proteins with spherical polyelectrolyte brushes in solution as studied by small-angle x-ray scattering. *Phys. Rev. E* **2004**, *70(6)*, 061403.

[50] Wittemann, A.; Ballauff, M. Interaction of proteins with linear polyelectrolytes and spherical polyelectrolyte brushes in aqueous solution. *Phys. Chem. Chem. Phys.* **2006**, *8(45)*, 5269-5275.

[51] Walkowiak, J.; Gradzielski, M.; Zauscher, S.; Ballauff, M. Interaction of proteins with a planar poly (acrylic acid) brush: analysis by quartz crystal microbalance with dissipation monitoring (QCM-D). *Polymers* **2020**, *13(1)*, 122.

[52] Cooper, C. L.; Dubin, P. L.; Kyaitmazer, A. B.; Turksen, S. Polyelectrolyte–protein complexes. *Curr. Opin. Colloid Interface Sci.* **2005**, *10(1-2)*, 52-78.

[53] Seyrek, E.; Dubin, P. L.; Tribet, C.; Gamble, E. A. Ionic strength dependence of protein-polyelectrolyte interactions. *Biomacromolecules* **2003**, *4(2)*, 273-282.

[54] Kyaitmazer, A. B.; Seeman, D.; Minsky, B. B.; Dubin, P. L.; Xu, Y. Protein–polyelectrolyte interactions. *Soft Matter* **2013**, *9(9)*, 2553-2583.

[55] Wittemann, A.; Haupt, B.; Ballauff, M. Adsorption of proteins on spherical polyelectrolyte brushes in aqueous solution. *Phys. Chem. Chem. Phys.* **2003**, *5(8)*, 1671-1677.

[56] Becker, A. L.; Henzler, K.; Welsch, N.; Ballauff, M.; Borisov, O. V. Proteins and polyelectrolytes: A charge relationship. *Curr. Opin. Colloid Interface Sci.* **2012**, *17(2)*, 90-96.

[57] Zheng, K., Chen, Y., Wang, X., Zhao, X., Qian, W., Xu, Y. Selective protein separation based on charge anisotropy by spherical polyelectrolyte brushes. *Langmuir* **2020**, *36(35)*, 10528-10536.

[58] Wittemann, A., Ballauff, M. Secondary structure analysis of proteins embedded in spherical polyelectrolyte brushes by FT-IR spectroscopy. *Anal. Chem.* **2004**, *76(10)*, 2813-2819.

[59] Hollmann, O., Czeslik, C. Characterization of a planar poly (acrylic acid) brush as a materials coating for controlled protein immobilization. *Langmuir* **2006**, *22(7)*, 3300-3305.

[60] Hollmann, O., Steitz, R., Czeslik, C. Structure and dynamics of α-lactalbumin adsorbed at a charged brush interface. *Phys. Chem. Chem. Phys.* **2008**, *10(10)*, 1448-1456.

[61] Wang, S., Chen, K., Xu, Y., Yu, X., Wang, W., Li, L., Guo, X. Protein immobilization and separation using anionic/cationic spherical polyelectrolyte brushes based on charge anisotropy. *Soft Matter* **2013**, *9(47)*, 11276-11287.

[62] Wang, S., Chen, K., Li, L., Guo, X. Binding between proteins and cationic spherical polyelectrolyte brushes: effect of pH, ionic strength, and stoichiometry. *Biomacromolecules* **2013**, *14(3)*, 818-827.

[63] Biesheuvel, P. M.; Wittemann, A. A modified box model including charged polyelectrolyte brush: Self-consistent field theory. *J.Phys.Chem. B* **2005**, *109*, 4209-4214.

[64] De Vos, W. M.; Leermakers, F. A. M.; De Keizer, A.; Cohen Stuart, M. A.; Klein J. M. Field theoretical analysis of driving forces for the uptake of proteins by like-charged polyelectrolyte brushes: effects of charge regulation and patchiness. *Langmuir* **2010**, *26(1)*, 249-259.

[65] Leermakers F. A. M.; Ballauff, M.; Borisov, O. V. On the mechanisms of interaction of globular proteins with polyelectrolyte brushes. *Langmuir* **2007**, *23(7)*, 237-247.

[66] Xu, X.; Angioletti-Uberti, S.; Lu, Y.; Dzubiella, J.; Ballauff, M. Interaction of proteins with polyelectrolytes: Comparison of theory to experiment. *Langmuir* **2018**, *35(16)*, 5373-5391.

[67] Kim, S.; Sureka, H. V.; Kayitmazer, A. B.; Wang, G.; Swan, J. W.; Olsen, B. D. Effect of protein surface charge distribution on protein-polyelectrolyte complexation. *Biomacromolecules* **2020**, *21(18)*, 3026-3037.

[68] Laktionov, M. Y.; Zhulina, E. B.; Borisov, O. V. Proteins and polyampholytes interacting with polyelectrolyte brushes and microgels: The charge reversal concept revised. *Langmuir* **2021**, *37(9)* 2865–2873.

[69] Salamatova T. O.; Laktionov, M. Y.; Zhulina, E. B.; Borisov, O. V. Polyelectrolyte Brush Interacting with Ampholytic Nanoparticles as Coarse-Grained Models of Globular Proteins: Poisson–Boltzmann Theory. *Biomacromolecules* **2023**, *24(6)* 2433-2446.

[70] Salamatova T. O.; Zhulina, E. B.; Borisov, O. V. Bovine Serum Albumin interaction with polyanionic and Polycationic brushes: the case theoretical study. *Int. J. Mol. Sci.* **2023**, *24(4)* 3395.

TOC Graphic

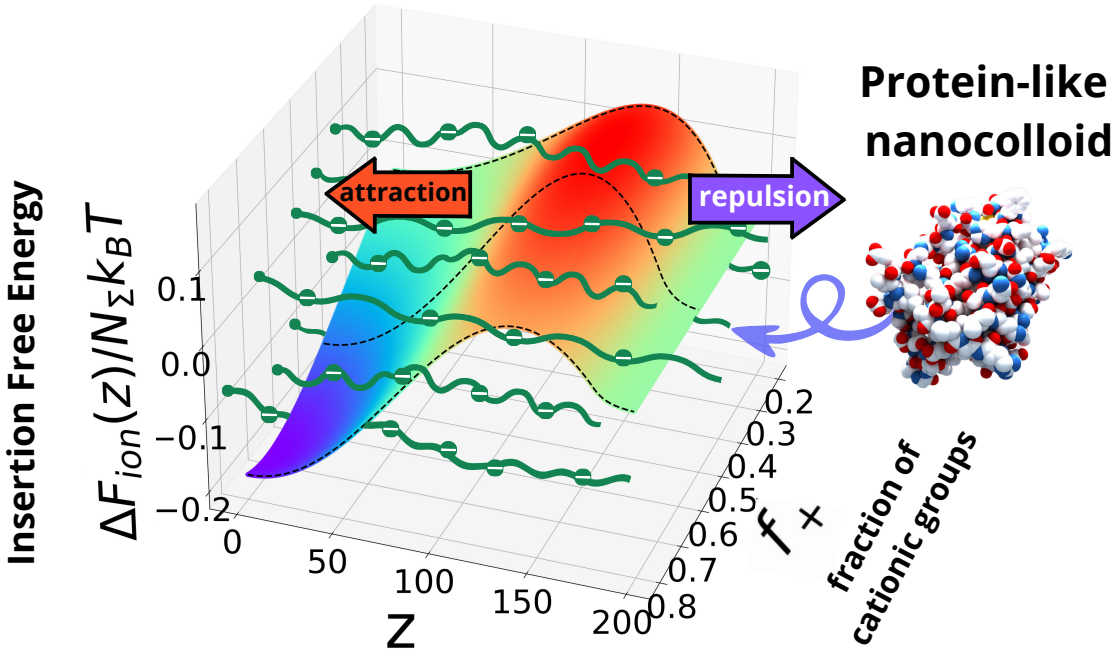
Protein-like
nanocolloid
attraction
repulsion
Insertion Free Energy
$\Delta F_{ion}(z)/N_\Sigma k_B T$
0.1
0.0
−0.1
−0.2
0
50
100
150
200
z
0.2
0.3
0.4
0.5
0.6
0.7
0.8
f
fraction of
cationic groups